

QED calculation of the nuclear magnetic shielding for hydrogen-like ions

V. A. Yerokhin,^{1,2,3} K. Pachucki,⁴ Z. Harman,^{1,2} and C. H. Keitel¹

¹Max Planck Institute for Nuclear Physics, Saupfercheckweg 1, D 69117 Heidelberg, Germany

²ExtreMe Matter Institute EMMI, GSI Helmholtzzentrum für

Schwerionenforschung, Planckstraße 1, D-64291 Darmstadt, Germany

³St. Petersburg State Polytechnical University, Polytekhnicheskaya 29, St. Petersburg 195251, Russia

⁴Faculty of Physics, University of Warsaw, Hoża 69, 00-681 Warsaw, Poland

We report an *ab initio* calculation of the shielding of the nuclear magnetic moment by the bound electron in hydrogen-like ions. This investigation takes into account several effects that have not been calculated before (electron self-energy, vacuum polarization, nuclear magnetization distribution), thus bringing the theory to the point where further progress is impeded by the uncertainty due to nuclear-structure effects. The QED corrections are calculated to all orders in the nuclear binding strength parameter and, independently, to the leading order in the expansion in this parameter. The results obtained lay the ground for the high-precision determination of nuclear magnetic dipole moments from measurements of the g -factor of hydrogen-like ions.

PACS numbers: 31.30.jn, 31.15.ac, 32.10.Dk, 21.10.Ky

I. INTRODUCTION

Last years showed much progress in the experimental determination of the g -factors of hydrogen-like ions [1–4]. Measurements, accurate up to a few parts in 10^{11} [4], were performed by studying a single ion confined in a Penning trap. These experiments provided the stringent tests of bound-state quantum electrodynamics (QED) theory and yielded the best determination of the electron mass [5].

In order to match the experimental accuracy, many sophisticated calculations were performed during the past years, in particular those of the one-loop self-energy [6–8], the one-loop vacuum-polarization [9], the nuclear recoil [10], and the two-loop QED effects [11, 12]. These calculations made it possible to determine the electron mass from the experimental values of the bound-electron g factor [13]. The theoretical accuracy of the bound-electron g factor in hydrogen-like ions is presently at the 10^{-11} level [12] for light elements up to carbon but deteriorates quickly for heavier elements because of the unknown higher-order two-loop QED effects scaling with the nuclear charge number Z as Z^5 .

The experimental investigations of the g -factors of hydrogen-like ions were so far performed for ions with spinless nuclei. However, when applied to the ions with a non-zero nuclear spin, such investigations can be useful as a new method for the determination of the magnetic dipole moments of the nuclei. This method has important advantages over the more traditional approaches, such as nuclear magnetic resonance (NMR), atomic beam magnetic resonance, collinear laser spectroscopy, and optical pumping (OP). These advantages are that (i) the simplicity of the system under investigation (a hydrogen-like ion) allows for an *ab initio* theoretical description with a reliable estimation of uncalculated effects and (ii) the influence of the nuclear-structure effects (which are the main limiting factors for theory) is relatively weak. This is in contrast to the existing methods, in which the

experimental data should be corrected for several physical effects, which are difficult to calculate. Among such effects is the diamagnetic shielding of the external magnetic field by the electrons in the atom. The NMR results should be also corrected for the paramagnetic chemical shift caused by the chemical environment [14] and the OP data are sensitive to the hyperfine mixing of the energy levels [15]. Significant (and generally unknown) uncertainties of calculations of these effects often lead to ambiguities in the published values of nuclear magnetic moments [16].

The goal of the present investigation is to perform an *ab initio* calculation of the g -factor of a hydrogen-like ion with a non-zero nuclear spin. It can be demonstrated that the nuclear-spin dependent part of the atomic g -factor can be parameterized in terms of the nuclear magnetic shielding constant σ , which describes the effective reduction of the coupling of the nuclear magnetic moment $\vec{\mu}$ to an external magnetic field \vec{B} caused by the shell electron(s),

$$-\vec{\mu} \cdot \vec{B} \rightarrow -\vec{\mu} \cdot \vec{B}(1 - \sigma). \quad (1)$$

The relativistic theory of the g -factor of a hydrogen-like ion with a non-zero nuclear spin (and, thus, the theory of the nuclear magnetic shielding) was examined in detail in Ref. [17]. In the present work, we go beyond the relativistic description of the nuclear magnetic shielding and calculate the dominant corrections to it, namely, the self-energy, the vacuum-polarization, and the nuclear magnetization distribution corrections. As a result, we bring the theory to the point where the uncertainty due to nuclear-structure effects impedes further progress.

The main challenge of the present work is the calculation of the self-energy correction. To the best of our knowledge, the only previous attempt to address it was made in Ref. [18]. In that work, the self-energy contribution to the shielding constant was estimated by the leading logarithm of its $Z\alpha$ expansion (where α is the

fine-structure constant). In our work, we calculate the self-energy correction rigorously to all orders in the binding nuclear strength parameter $Z\alpha$ and, independently, perform an analytical calculation to the leading order in the expansion in this parameter (including both the logarithm and constant terms). First results of this work were reported in Ref. [19].

The rest of the paper is organized as follows. In Sec. II we summarize the relativistic theory of the g -factor of an ion with a non-zero nuclear spin and the theory of the nuclear magnetic shielding. Our calculation of the self-energy and vacuum-polarization corrections to all orders in $Z\alpha$ is described in Sec. III. In Sec. IV we report the calculation of the QED correction to the nuclear magnetic shielding to the leading order in the $Z\alpha$ expansion. Sec. V deals with the other effects, namely, the nuclear magnetization distribution, the nuclear recoil, and the quadrupole interaction. Numerical results and discussion are given in Sec. VI. The paper ends with conclusion in Sec. VII.

The relativistic units ($m = \hbar = c = 1$) and the charge units $\alpha = e^2/(4\pi)$ are used throughout this paper.

II. LEADING-ORDER MAGNETIC SHIELDING

We consider a hydrogen-like ion with a non-zero spin nucleus placed in a weak homogenous magnetic field \vec{B} directed along the z axis. Assuming that the energy shift due to the interaction with the \vec{B} field (the Zeeman shift) is much smaller than the hyperfine-structure splitting (hfs), the energy shift can be expressed in terms of the g factor of the atomic system g_F ,

$$\Delta E = g_F \mu_0 B M_F, \quad (2)$$

where $B = |\vec{B}|$, $\mu_0 = |e|/(2m)$ is the Bohr magneton, e and m are the elementary charge and the electron mass, respectively, and M_F is the z projection of the total angular momentum of the system F . To the leading order, the energy shift is given by

$$\Delta E = \langle FM_F | \left[-\frac{e}{2} (\vec{r} \times \vec{\alpha}) \cdot \vec{B} - \vec{\mu} \cdot \vec{B} \right] | FM_F \rangle, \quad (3)$$

where $|FM_F\rangle \equiv |jIM_F\rangle$ is the wave function of the ion, j and I are the angular momentum quantum numbers of the electron and nucleus, respectively; $\vec{\mu}$ is the operator of the magnetic moment of the nucleus. The matrix element (3) can easily be evaluated, yielding the well-known leading-order relativistic result [21],

$$g_F^{(0)} = g_j^{(0)} \frac{\langle \vec{j} \cdot \vec{F} \rangle}{F(F+1)} - \frac{m}{m_p} g_I \frac{\langle \vec{I} \cdot \vec{F} \rangle}{F(F+1)}, \quad (4)$$

where $g_j^{(0)}$ is the Dirac bound-electron g factor [20], $g_I = \mu/(\mu_N I)$ is the nuclear g factor, $\mu = \langle II | \vec{\mu} | II \rangle$ is the nuclear magnetic moment, $\mu_N = |e|/(2m_p)$ is the nuclear

magneton, m_p is the proton mass, and $\langle \vec{j} \cdot \vec{F} \rangle$ and $\langle \vec{I} \cdot \vec{F} \rangle$ are the angular-momentum recoupling coefficients,

$$\langle \vec{j} \cdot \vec{F} \rangle = [F(F+1) - I(I+1) + j(j+1)]/2, \quad (5)$$

$$\langle \vec{I} \cdot \vec{F} \rangle = [F(F+1) + I(I+1) - j(j+1)]/2. \quad (6)$$

Generalizing the leading-order result to include the higher-order correction, we write the atomic g factor g_F as

$$g_F = g_j \frac{\langle \vec{j} \cdot \vec{F} \rangle}{F(F+1)} - \frac{m}{m_p} g_I (1 - \sigma) \frac{\langle \vec{I} \cdot \vec{F} \rangle}{F(F+1)}. \quad (7)$$

In the above equation, the bound-electron g factor $g_j = g_j^{(0)} + \alpha/(2\pi) + \dots$ incorporates all corrections that do not depend on the nuclear spin, whereas the nuclear shielding constant σ parameterizes the nuclear-spin dependent corrections. The bound-electron g factor g_j has been extensively studied during the last years, both theoretically [8–12] and experimentally [1–3]. The goal of the present work is the *ab initio* theoretical description of the nuclear shielding parameter σ .

It can be seen from Eq. (7) that the nuclear-spin dependent contribution to the atomic g factor g_F is suppressed by the electron-to-proton mass ratio and thus is by about three orders of magnitude smaller than the nuclear-spin independent part proportional to g_j . It is, however, possible to form a combination of the atomic g factors which is free of the nuclear-spin independent contributions. So, for ions with the nuclear spin $I > 1/2$, we introduce the sum of the atomic g factors \bar{g} that is directly proportional to the nuclear magnetic moment,

$$\bar{g} \equiv g_{F=I+1/2} + g_{F=I-1/2} = -2 \frac{m}{m_p} \frac{\mu}{\mu_N I} (1 - \sigma). \quad (8)$$

This combination of the g factors is particularly convenient for the determination of the nuclear magnetic dipole moments from experiment. Indeed, if both the $g_{F=I+1/2}$ and $g_{F=I-1/2}$ g -factors are measured and σ is known from theory, Eq. (8) determines the nuclear magnetic moment μ . For the ions with a nuclear spin $I = 1/2$, Eq. (8) is not applicable and the nuclear magnetic moment should be determined from Eq. (7).

Contributions to the nuclear magnetic shielding are described by Feynman diagrams with two external interactions, one with the external magnetic field (the Zeeman interaction),

$$V_{\text{zee}}(r) = \frac{|e|}{2} \vec{B} \cdot (\vec{r} \times \vec{\alpha}), \quad (9)$$

and another, with the magnetic dipole field of the nucleus (the hfs interaction)

$$V_{\text{hfs}}(r) = \frac{|e|}{4\pi} \vec{\mu} \cdot \frac{\vec{r} \times \vec{\alpha}}{r^3}. \quad (10)$$

The leading-order contribution to the magnetic shielding comes from the following energy shift

$$\Delta E = 2 \sum_{n \neq a} \frac{1}{\varepsilon_a - \varepsilon_n} \langle a | V_{\text{zee}} | n \rangle \langle n | V_{\text{hfs}} | a \rangle, \quad (11)$$

where the summation runs over the whole Dirac spectrum with the reference state excluded. As follows from Eqs. (2) and (7), contributions to the shielding constant $\delta\sigma$ are obtained from the corresponding energy shifts δE by

$$\delta\sigma = \frac{\delta E}{\mu B M_F \frac{\langle \vec{r} \cdot \vec{F} \rangle}{IF(F+1)}}. \quad (12)$$

For the electronic states with $j_a = 1/2$, all nuclear quantum numbers in Eq. (11) can be factorized out. The expression for the shielding constant is then obtained from that formula by using the following substitutions

$$\begin{aligned} V_{zee} &\rightarrow \tilde{V}_{zee} \equiv (\vec{r} \times \vec{\alpha})_0, & V_{hfs} &\rightarrow \tilde{V}_{hfs} \equiv \frac{(\vec{r} \times \vec{\alpha})_0}{r^3}, \\ |a\rangle &\rightarrow |a_{1/2}\rangle, & |n\rangle &\rightarrow |n_{1/2}\rangle, \\ 2 &\rightarrow \alpha \text{ (prefactor)}, \end{aligned} \quad (13)$$

where the zero subscript refers to the zero spherical component of the vector. Here and in what follows, $|n_{1/2}\rangle \equiv |\kappa_n, \mu_n = 1/2\rangle$ denotes the Dirac state with the relativistic angular quantum number κ_n and the fixed momentum projection $\mu_n = 1/2$.

So, for $j_a = 1/2$, the leading contribution to the magnetic shielding is given by a simple expression

$$\sigma^{(0)} = \alpha \sum_{n \neq a} \frac{1}{\varepsilon_a - \varepsilon_n} \langle a_{1/2} | \tilde{V}_{zee} | n_{1/2} \rangle \langle n_{1/2} | \tilde{V}_{hfs} | a_{1/2} \rangle. \quad (14)$$

Performing the angular integrations with help of Eq. (A3), one gets for the ns reference state

$$\sigma^{(0)} = \alpha \sum_{\kappa_n = -1, 2} x_{\kappa_n}^2 \sum_{n \neq a} \frac{R_{an}^{(1)} R_{na}^{(-2)}}{\varepsilon_a - \varepsilon_n}, \quad (15)$$

where $R^{(\alpha)}$ are the radial integrals of the form

$$R_{ab}^{(\alpha)} = \int_0^\infty dr r^{2+\alpha} [g_a(r) f_b(r) + f_a(r) g_b(r)], \quad (16)$$

$g(r)$ and $f(r)$ are the upper and lower radial components of the Dirac wave function, respectively, and the angular prefactors x_{κ_n} are given by $x_{\kappa_n = -1} = -2/3$, $x_{\kappa_n = 2} = -\sqrt{2}/3$.

For the point nuclear model, the sum over the Dirac spectrum in the above expression can be evaluated analytically [22–24], see also more recent studies [17, 25],

$$\begin{aligned} \sigma^{(0)} &= -\frac{4\alpha Z\alpha}{9} \left(\frac{1}{3} - \frac{1}{6(1+\gamma)} + \frac{2}{\gamma} - \frac{3}{2\gamma-1} \right) \\ &= \alpha Z\alpha \left(\frac{1}{3} + \frac{97}{108}(Z\alpha)^2 + \dots \right), \end{aligned} \quad (17)$$

where $\gamma = \sqrt{1 - (Z\alpha)^2}$. For the extended nucleus, the calculation is easily performed numerically [17].

III. QED CORRECTION

A. Self-energy: General formulas

The self-energy correction in the presence of the external magnetic field and the magnetic dipole field of the nucleus is graphically represented by six topologically non-equivalent Feynman diagrams shown in Fig. 1. General expressions for these diagrams are conveniently obtained by using the two-time Green's function method [26]. The resulting formulas are summarized below.

1. Perturbed-orbital contribution

The irreducible contributions of diagrams on Figs. 1(a)-(c) can be represented in terms of the one-loop self-energy operator Σ . This part will be termed as the perturbed-orbital contribution. The corresponding energy shift is

$$\begin{aligned} \Delta E_{po} &= 2 \langle \Sigma_R \frac{1}{(\varepsilon_a - H)'} V_{zee} \frac{1}{(\varepsilon_a - H)'} V_{hfs} \rangle \\ &+ 2 \langle \Sigma_R \frac{1}{(\varepsilon_a - H)'} V_{hfs} \frac{1}{(\varepsilon_a - H)'} V_{zee} \rangle \\ &- 2 \langle \Sigma_R \frac{1}{(\varepsilon_a - H)^{2'}} V_{zee} \rangle \langle V_{hfs} \rangle \\ &- 2 \langle \Sigma_R \frac{1}{(\varepsilon_a - H)^{2'}} V_{hfs} \rangle \langle V_{zee} \rangle \\ &- 2 \langle \Sigma_R \rangle \langle V_{zee} \frac{1}{(\varepsilon_a - H)^{2'}} V_{hfs} \rangle \\ &+ 2 \langle V_{zee} \frac{1}{(\varepsilon_a - H)'} \Sigma_R \frac{1}{(\varepsilon_a - H)'} V_{hfs} \rangle, \end{aligned} \quad (18)$$

where we used the short-hand notations for the reduced Green's function,

$$\frac{1}{(\varepsilon_a - H)'} = \sum_{n \neq a} \frac{|n\rangle \langle n|}{\varepsilon_a - \varepsilon_n}, \quad (19)$$

and its derivative

$$\frac{1}{(\varepsilon_a - H)^{2'}} = \sum_{n \neq a} \frac{|n\rangle \langle n|}{(\varepsilon_a - \varepsilon_n)^2}. \quad (20)$$

The (unrenormalized) self-energy operator $\Sigma(\varepsilon)$ is defined by its matrix elements as follows

$$\langle i | \Sigma(\varepsilon) | k \rangle = \frac{i}{2\pi} \int_{-\infty}^{\infty} d\omega \sum_n \frac{\langle in | I(\omega) | nk \rangle}{\varepsilon - \omega - u \varepsilon_n}, \quad (21)$$

where $I(\omega)$ is the operator of the electron-electron interaction, $I(\omega) = e^2 \alpha_\mu \alpha_\nu D^{\mu\nu}(\omega)$, $D^{\mu\nu}(\omega)$ is the photon propagator, α_μ are the Dirac matrices, and $u \equiv 1 - i0$, where $i0$ is a small imaginary addition that defines the

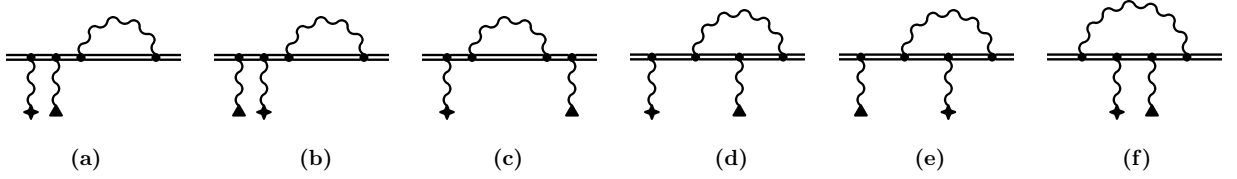


FIG. 1: Self-energy correction to the nuclear magnetic shielding. Double line represents the electron in the binding nuclear field. The wave line terminated by a triangle represents the dipole hyperfine interaction with the nucleus and the wave line terminated by a cross represents the interaction with the external magnetic field.

positions of the poles of the electron propagators with respect to the integration contour. The summation over n runs over the complete Dirac spectrum. Renormalization of the one-loop self-energy operator is well described in the literature, see, e.g., Ref. [27]. In this work, the renormalized part of the self-energy operator is defined as

$$\Sigma_R(\varepsilon) = \Sigma(\varepsilon) - \beta \delta m - (\varepsilon - \vec{\alpha} \cdot \vec{p} - V_C - \beta m) B^{(1)}, \quad (22)$$

where δm is the mass counterterm, β is the Dirac β matrix, $B^{(1)}$ is the one-loop renormalization constant, V_C is the binding Coulomb potential of the nucleus, and the renormalization is to be performed in momentum space with a covariant regularization of ultraviolet (UV) divergencies. Details on the renormalization procedure and explicit formulas for $\Sigma_R(\varepsilon)$ can be found in Refs. [28, 29].

2. Single-vertex contributions

The irreducible contribution of the diagram shown in Fig. 1(d), together with the corresponding derivative term, is referred to as the *hfs-vertex* contribution. It is given by

$$\Delta E_{\text{vr,hfs}} = 2 \langle \Gamma_{\text{hfs},R} \frac{1}{(\varepsilon_a - H)'} V_{\text{zee}} \rangle + 2 \langle \Sigma'_R \frac{1}{(\varepsilon_a - H)'} V_{\text{zee}} \rangle \langle V_{\text{hfs}} \rangle, \quad (23)$$

where $\Gamma_{\text{hfs},R} \equiv \Gamma_{\text{hfs},R}(\varepsilon_a)$ is the renormalized part of the 3-point vertex representing the interaction with the hfs field and $\Sigma'_R \equiv \Sigma'_R(\varepsilon_a)$ is the derivative of the renormalized self-energy operator over the energy argument, $\Sigma'_R(\varepsilon_a) = d/(d\varepsilon) \Sigma_R(\varepsilon)|_{\varepsilon=\varepsilon_a}$. The unrenormalized 3-point hfs vertex operator is defined by its matrix elements as

$$\langle i | \Gamma_{\text{hfs}}(\varepsilon) | k \rangle = \frac{i}{2\pi} \int_{-\infty}^{\infty} d\omega \times \sum_{n_1 n_2} \frac{\langle i n_2 | I(\omega) | n_1 k \rangle \langle n_1 | V_{\text{hfs}} | n_2 \rangle}{(\varepsilon - \omega - u\varepsilon_{n_1})(\varepsilon - \omega - u\varepsilon_{n_2})}. \quad (24)$$

The renormalized part of the operator is obtained as

$$\Gamma_{\text{hfs},R}(\varepsilon) = \Gamma_{\text{hfs}}(\varepsilon) - V_{\text{hfs}} L^{(1)}, \quad (25)$$

where $L^{(1)}$ is the one-loop renormalization constant and the renormalization is to be performed in momentum space with a covariant regularization of UV divergencies, see Ref. [29] for details.

The irreducible contribution of the diagram shown in Fig. 1(e), together with the corresponding derivative term, is referred to as the *Zeeman-vertex* contribution. It is given by

$$\Delta E_{\text{vr,zee}} = 2 \langle \Gamma_{\text{zee},R} \frac{1}{(\varepsilon_a - H)'} V_{\text{hfs}} \rangle + 2 \langle \Sigma'_R \frac{1}{(\varepsilon_a - H)'} V_{\text{hfs}} \rangle \langle V_{\text{zee}} \rangle, \quad (26)$$

where the 3-point Zeeman vertex is defined analogously to the hfs one.

3. Double-vertex contribution

The contribution of the diagram shown on Fig. 1(f), together with the corresponding derivative terms, will be termed as the *double-vertex* contribution. It is defined by

$$\Delta E_{\text{d,vr}} = 2 \langle \Lambda(\varepsilon_a) \rangle + \langle \Sigma'' \rangle \langle V_{\text{zee}} \rangle \langle V_{\text{hfs}} \rangle + \langle \Gamma'_{\text{hfs}} \rangle \langle V_{\text{zee}} \rangle + \langle \Gamma'_{\text{zee}} \rangle \langle V_{\text{hfs}} \rangle - 2 \langle V_{\text{zee}} \frac{1}{(\varepsilon_a - H)'} V_{\text{hfs}} \rangle \frac{i}{2\pi} \int_{-\infty}^{\infty} d\omega \sum_{a'} \frac{\langle a a' | I(\omega) | a' a \rangle}{(-\omega + i0)^2}, \quad (27)$$

where Λ denotes the 4-point vertex representing the interaction with both the Zeeman and hfs interactions,

$$\langle i | \Lambda(\varepsilon) | k \rangle = \frac{i}{2\pi} \int_{-\infty}^{\infty} d\omega \times \sum_{n_1 n_2 n_3} \frac{\langle i n_3 | I(\omega) | n_1 k \rangle \langle n_1 | V_{\text{zee}} | n_2 \rangle \langle n_2 | V_{\text{hfs}} | n_3 \rangle}{(\varepsilon - \omega - u\varepsilon_{n_1})(\varepsilon - \omega - u\varepsilon_{n_2})(\varepsilon - \omega - u\varepsilon_{n_3})}, \quad (28)$$

$\Sigma'' \equiv \Sigma''(\varepsilon_a)$ denotes the second derivative of the self-energy operator over the energy argument, $\Sigma''(\varepsilon_a) = d^2/(d^2\varepsilon) \Sigma(\varepsilon)|_{\varepsilon=\varepsilon_a}$, $\Gamma' \equiv \Gamma'(\varepsilon_a)$ denotes the derivative of the vertex operator over the energy argument, and a' denotes the intermediate electron states with the energy $\varepsilon_{a'} = \varepsilon_a$. The last term in Eq. (27) is added artificially, in order to make the whole expression for $\Delta E_{\text{d,vr}}$ infrared

(IR) finite. The same term will be subtracted from the derivative contribution defined below, see Eq. (29).

We note that all terms in Eq. (27) are UV finite, so that there is no need for any UV regularization. There are, however, IR divergences, which appear when the energy of the intermediate electron states in the electron propagators coincides with the energy of the reference state. The divergences cancel out in the sum of individual terms in Eq. (27).

4. Derivative contribution

Finally, the remaining contribution will be termed as the *derivative* term. It is given by

$$\Delta E_{\text{der}} = 2 \left[\langle \Sigma'_R \rangle + \frac{i}{2\pi} \int_{-\infty}^{\infty} d\omega \sum_{a'} \frac{\langle aa' | I(\omega) | a'a \rangle}{(-\omega + i0)^2} \right] \times \langle V_{\text{zee}} \frac{1}{(\varepsilon_a - H)'} V_{\text{hfs}} \rangle. \quad (29)$$

The second term in the brackets is added artificially, in order to compensate the IR reference-state divergence present in the first term, making the total expression for ΔE_{der} IR finite. Note that this term is exactly the same as the one added to Eq. (27) but has the opposite sign.

Finally, the total self-energy correction is given by the sum of the contributions discussed above,

$$\Delta E_{\text{SE}} = \Delta E_{\text{po}} + \Delta E_{\text{vr,hfs}} + \Delta E_{\text{vr,zee}} + \Delta E_{\text{d,vr}} + \Delta E_{\text{der}}, \quad (30)$$

which are given by Eqs. (18), (23), (26), (27), and (29), respectively.

B. Self-energy: Calculation

The general formulas reported so far represent contributions to the energy shift. We now have to separate out the nuclear degrees of freedom and convert the corrections to the energy into corrections to the shielding constant. In most cases, this is achieved simply by using the substitutions (13). The double-vertex contribution, however, requires an explicit angular-momentum algebra calculation for the separation of the nuclear variables.

We will see that most of the corrections to the shielding constant can be regarded as generalizations of the corrections already discussed in the literature. So, our present calculation will be largely based on the previous investigations of the self-energy correction to the Lamb shift [28, 30], to the hyperfine structure [31–33], and to the g factor [32–34]. The double-vertex correction of the kind similar to that in the present work appeared in the evaluation of the self-energy correction to the parity-nonconserving transitions in Refs. [35, 36]. However, in this work we develop a different scheme for the evaluation of the double-vertex contribution based on the analytical representation of the Dirac-Coulomb Green function.

1. Perturbed-orbital contributions

The matrix elements of the self-energy operator are diagonal in the relativistic angular momentum quantum number κ and the momentum projection μ . Because of this, the angular reduction of the perturbed-orbital contribution is achieved by the same set of substitutions (13) as for the leading-order magnetic shielding. The resulting contribution to the shielding constant is conveniently represented as

$$\Delta \sigma_{\text{po}} = \alpha \langle a_{1/2} | \Sigma_R(\varepsilon_a) | \delta^{(2)} a_{1/2} \rangle + \alpha \langle \delta_{\text{hfs}}^{(1)} a_{1/2} | \Sigma_R(\varepsilon_a) | \delta_{\text{zee}}^{(1)} a_{1/2} \rangle, \quad (31)$$

where the first-order perturbations of the reference-state wave function are given by

$$|\delta_{\text{hfs}}^{(1)} a_{1/2}\rangle = \sum_{n \neq a} |n_{1/2}\rangle \frac{1}{\varepsilon_a - \varepsilon_n} \langle n_{1/2} | \tilde{V}_{\text{hfs}} | a_{1/2} \rangle, \quad (32)$$

and

$$|\delta_{\text{zee}}^{(1)} a_{1/2}\rangle = \sum_{n \neq a} |n_{1/2}\rangle \frac{1}{\varepsilon_a - \varepsilon_n} \langle n_{1/2} | \tilde{V}_{\text{zee}} | a_{1/2} \rangle, \quad (33)$$

and $|\delta^{(2)} a\rangle$ is the standard second-order perturbation [37] of the reference-state wave function induced by *both* interactions, \tilde{V}_{hfs} and \tilde{V}_{zee} . Note that only the diagonal in κ part of the perturbed wave functions contributes to $\Delta \sigma_{\text{po}}$. The calculation of the non-diagonal matrix elements of the self-energy operator is performed by a straightforward generalization of the method developed in Ref. [30] for the first-order self-energy correction to the Lamb shift.

2. Hfs-vertex contributions

The hfs-vertex correction to the energy shift (23) for the reference state with $j_a = 1/2$ can be converted to the correction to the magnetic shielding by the substitution (13). The result is

$$\Delta \sigma_{\text{vr,hfs}} = \frac{i\alpha}{2\pi} \int_{-\infty}^{\infty} d\omega \times \sum_{n_1 n_2} \frac{\langle a_{1/2} n_2 | I(\omega) | n_1 \delta_{\text{zee}}^{(1)} a_{1/2} \rangle \langle n_1 | \tilde{V}_{\text{hfs}} | n_2 \rangle}{(\varepsilon_a - \omega - u \varepsilon_{n_1})(\varepsilon_a - \omega - u \varepsilon_{n_2})} - \langle \tilde{V}_{\text{hfs}} \rangle \frac{i\alpha}{2\pi} \int_{-\infty}^{\infty} d\omega \sum_n \frac{\langle a_{1/2} n | I(\omega) | n \delta_{\text{zee}}^{(1)} a_{1/2} \rangle}{(\varepsilon_a - \omega - u \varepsilon_n)^2}, \quad (34)$$

where the covariant regularization of the ultraviolet (UV) divergences is implicitly assumed. The right-hand-side of Eq. (34) differs from the vertex and reducible parts of the self-energy correction to the hyperfine structure only by the perturbed wave function $|\delta_{\text{zee}}^{(1)} a\rangle$ in place of one of the

reference-state wave functions $|a\rangle$. The main complication brought by this difference is that the perturbed wave function contains components with different values of the relativistic angular quantum number κ . So, for the reference state with $\kappa_a = -1$, the perturbed wave function has components with $\kappa = -1$ and $\kappa = 2$, both of which contribute to the first term in Eq. (34), denoted in the following as $\Delta\sigma_{\text{ver,hfs}}$. The second (reducible) term contains only the $\kappa = \kappa_a$ component of the perturbed wave function and its calculation is done exactly as described in Ref. [31]. Below, we present the generalization of formulas derived in Ref. [31, 33] needed for the evaluation of $\Delta\sigma_{\text{ver,hfs}}$.

As explained in Ref. [31], the covariant separation of the UV divergences is conveniently performed by dividing the vertex contribution into the zero- and many-potential parts, according to the number of interactions with the binding Coulomb field in the electron propagator,

$$\Delta\sigma_{\text{ver,hfs}} = \Delta\sigma_{\text{ver,hfs}}^{(0)} + \Delta\sigma_{\text{ver,hfs}}^{(1+)} . \quad (35)$$

The zero-potential part is calculated in momentum space with the dimensional regularization of the UV divergences. The Fourier transform of the \tilde{V}_{hfs} is done by

$$\frac{(\vec{r} \times \vec{\alpha})_0}{r^3} \rightarrow (-4\pi i) \frac{(\vec{q} \times \vec{\alpha})_0}{\vec{q}^2} , \quad (36)$$

where $\vec{q} = \vec{p}_1 - \vec{p}_2$ is the transferred momentum. The contribution of the zero-potential hfs vertex part to the

shielding constant is

$$\Delta\sigma_{\text{ver,hfs}}^{(0)} = -4\pi i\alpha \int \frac{d\vec{p}_1}{(2\pi)^3} \frac{d\vec{p}_2}{(2\pi)^3} \times \bar{\psi}_{a_{1/2}}(\vec{p}_1) \frac{[\vec{q} \times \vec{\Gamma}_R(p_1, p_2)]_0}{\vec{q}^2} \psi_{\delta a_{1/2}}(\vec{p}_2) , \quad (37)$$

where p_1 and p_2 are 4-vectors with the fixed time component $p_1 = (\varepsilon_a, \vec{p}_1)$, $p_2 = (\varepsilon_a, \vec{p}_2)$, ψ_a and $\psi_{\delta a}$ are the reference-state and the perturbed wave functions, respectively, $\bar{\psi} = \psi^\dagger \gamma^0$ is the Dirac conjugation, and $\vec{\Gamma}_R$ is the renormalized one-loop vertex operator [28]. For evaluating the integrals over the angular variables, it is convenient to use the following representation of the vertex operator sandwiched between the Dirac wave functions

$$\begin{aligned} \bar{\psi}_a(\vec{p}_1) \vec{\Gamma}_R(p_1, p_2) \psi_b(\vec{p}_2) &= \frac{\alpha}{4\pi} \left[\mathcal{R}_1 \chi_{\kappa_a \mu_a}^\dagger(\hat{p}_1) \vec{\sigma} \chi_{-\kappa_b \mu_b}(\hat{p}_2) \right. \\ &+ \mathcal{R}_2 \chi_{-\kappa_a \mu_a}^\dagger(\hat{p}_1) \vec{\sigma} \chi_{\kappa_b \mu_b}(\hat{p}_2) \\ &+ (\mathcal{R}_3 \vec{p}_1 + \mathcal{R}_4 \vec{p}_2) \chi_{\kappa_a \mu_a}^\dagger(\hat{p}_1) \chi_{\kappa_b \mu_b}(\hat{p}_2) \\ &\left. + (\mathcal{R}_5 \vec{p}_1 + \mathcal{R}_6 \vec{p}_2) \chi_{-\kappa_a \mu_a}^\dagger(\hat{p}_1) \chi_{-\kappa_b \mu_b}(\hat{p}_2) \right] , \quad (38) \end{aligned}$$

where $\hat{p} \equiv \vec{p}/|\vec{p}|$, $\chi_{\kappa\mu}(\hat{p})$ are the spin-angular Dirac spinors [38], and the scalar functions \mathcal{R}_i are given by Eqs. (A7)–(A12) of Ref. [39]. Integration over the angular variables yields (cf. Eq. (30) of Ref. [33])

$$\begin{aligned} \Delta\sigma_{\text{ver,hfs}}^{(0)} &= -\frac{\alpha^2}{48\pi^5} \sum_{\kappa_{\delta a}} x_{\kappa_{\delta a}} i^{l_a - l_{\delta a}} \int_0^\infty dp_{1r} dp_{2r} \int_{|p_{1r} - p_{2r}|}^{p_{1r} + p_{2r}} dq_r \frac{p_{1r} p_{2r}}{q_r} \\ &\times \left\{ \mathcal{R}_1 [p_{1r} K_1(\kappa_a, -\kappa_{\delta a}) - p_{2r} K_1'(\kappa_a, -\kappa_{\delta a})] + \mathcal{R}_2 [p_{1r} K_1(-\kappa_a, \kappa_{\delta a}) - p_{2r} K_1'(-\kappa_a, \kappa_{\delta a})] \right. \\ &\left. + p_{1r} p_{2r} (\mathcal{R}_3 + \mathcal{R}_4) K_2(\kappa_a, \kappa_{\delta a}) + p_{1r} p_{2r} (\mathcal{R}_5 + \mathcal{R}_6) K_2(-\kappa_a, -\kappa_{\delta a}) \right\} , \quad (39) \end{aligned}$$

where $p_{i_r} = |\vec{p}_i|$, $q_r = |\vec{q}|$, $\kappa_{\delta a}$ is the relativistic angular quantum number of the perturbed wave function, $l_n = |\kappa_n + 1/2| - 1/2$, $x_{\kappa=-1} = -2/3$, $x_{\kappa=2} = -\sqrt{2}/3$, and the basic angular integrals $K_i(\kappa, \kappa')$ are defined and evaluated in Appendix A.

The many-potential vertex contribution is free from UV divergences and thus can be calculated in coordinate space. The result after the integration over the angular

variables is

$$\begin{aligned} \Delta\sigma_{\text{ver,hfs}}^{(1+)} &= \sum_{\kappa_{\delta a}=-1,2} x_{\kappa_{\delta a}} \frac{i\alpha^2}{2\pi} \int_{-\infty}^\infty d\omega \\ &\times \sum_{n_1 n_2} \frac{R_{n_1 n_2}^{(-2)} \sum_J X_J(\kappa_1, \kappa_2) R_J(\omega, a n_2 n_1 \delta a)}{(\varepsilon - \omega - u \varepsilon_{n_1})(\varepsilon - \omega - u \varepsilon_{n_2})} \\ &- \text{subtraction} , \quad (40) \end{aligned}$$

where $R_{n_1 n_2}^{(-2)}$ is the radial integral of the hfs type given

by Eq. (16), X_J is the angular coefficient,

$$X_J(\kappa_1, \kappa_2) = \frac{(-1)^{j_{\delta a}-1/2}}{\sqrt{2}} \begin{Bmatrix} j_1 & j_2 & 1 \\ j_{\delta a} & j_a & J \end{Bmatrix} \times \frac{-\kappa_1 - \kappa_2}{\sqrt{3}} C_1(-\kappa_2, \kappa_1), \quad (41)$$

$C_1(\kappa_a, \kappa_b)$ is the reduced matrix element of the normalized spherical harmonics given by Eq. (C10) of Ref. [28], R_J is the relativistic generalization of the Slater radial integral given by Eqs. (C1)–(C9) of Ref. [28], and the subtraction in the last line of Eq. (40) means that the contribution of the free propagators (already accounted for by the zero-potential term) needs to be subtracted.

3. Zeeman-vertex contribution

The Zeeman-vertex correction to the energy shift (26) for the reference state with $j_a = 1/2$ can be converted to the correction to the magnetic shielding by the substitution (13). The result has the form analogous to that for the hfs-vertex contribution,

$$\Delta\sigma_{\text{vr},\text{zee}} = \frac{i\alpha}{2\pi} \int_{-\infty}^{\infty} d\omega \times \sum_{n_1 n_2} \frac{\langle a_{1/2} n_2 | I(\omega) | n_1 \delta_{\text{hfs}}^{(1)} a_{1/2} \rangle \langle n_1 | \tilde{V}_{\text{zee}} | n_2 \rangle}{(\varepsilon_a - \omega - u \varepsilon_{n_1})(\varepsilon_a - \omega - u \varepsilon_{n_2})} - \langle \tilde{V}_{\text{zee}} \rangle \frac{i\alpha}{2\pi} \int_{-\infty}^{\infty} d\omega \sum_n \frac{\langle a_{1/2} n | I(\omega) | n \delta_{\text{hfs}}^{(1)} a_{1/2} \rangle}{(\varepsilon_a - \omega - u \varepsilon_n)^2}, \quad (42)$$

where the covariant regularization of the UV divergences is implicitly assumed. The above expression looks very similar to Eq. (34) and can be evaluated almost in the same way, except for the zero-potential vertex contribution. The expression for the zero-potential Zeeman vertex contribution is different from the hfs case because the momentum representation of the interaction with a constant magnetic field involves a δ -function. The diagonal matrix element of the Zeeman vertex operator was evaluated previously in Ref. [34]; here we present the generalization of the formulas required for the non-diagonal case.

The Fourier transform of the interaction with the external magnetic field is given by

$$\vec{B} \times \vec{r} \rightarrow -i(2\pi)^3 \vec{B} \times \vec{\nabla}_{\vec{p}'} \delta^3(\vec{p} - \vec{p}'). \quad (43)$$

The contribution of the zero-potential vertex to the shielding constant is

$$\Delta\sigma_{\text{ver},\text{zee}}^{(0)} = -i\alpha \int \frac{d\vec{p} d\vec{p}'}{(2\pi)^3} \bar{\psi}_{a_{1/2}}(\vec{p}) \times \left[\vec{\nabla}_{\vec{p}'} \delta^3(\vec{p} - \vec{p}') \times \vec{\Gamma}_R(p, p') \right]_0 \psi_{\delta a_{1/2}}(\vec{p}'), \quad (44)$$

where the gradient $\vec{\nabla}_{\vec{p}'}$ acts on the δ -function only. This expression is transformed by integrating by parts and carrying out the integration with the δ -function analytically. The result after the angular integration consists of two parts (cf. Eqs. (27) and (36) of Ref. [34]),

$$\Delta\sigma_{\text{ver},\text{zee}}^{(0)} = \Delta\sigma_{\text{ver},\text{zee},1}^{(0)} + \Delta\sigma_{\text{ver},\text{zee},2}^{(0)}, \quad (45)$$

where

$$\Delta\sigma_{\text{ver},\text{zee},1}^{(0)} = \frac{\alpha^2}{\pi} \sum_{\kappa_{\delta a}} x_{\kappa_{\delta a}} i^{l_a - l_{\delta a}} \int_0^\infty \frac{p^2 dp}{8\pi^3} A(\rho) \times \left[g_a \tilde{g}_{\delta a} A_1(\kappa_a, \kappa_{\delta a}) + f_a \tilde{f}_{\delta a} A_1(-\kappa_a, -\kappa_{\delta a}) - p g_a f_{\delta a} A_2(\kappa_a, -\kappa_{\delta a}) - p f_a g_{\delta a} A_2(-\kappa_a, \kappa_{\delta a}) \right], \quad (46)$$

and

$$\Delta\sigma_{\text{ver},\text{zee},2}^{(0)} = -\frac{\alpha^2}{4\pi} \sum_{\kappa_{\delta a}} x_{\kappa_{\delta a}} i^{l_a - l_{\delta a}} \int_0^\infty \frac{p^2 dp}{8\pi^3} \times \left\{ b_1(\rho) [g_a f'_{\delta a} A_2(\kappa_a, -\kappa_{\delta a}) + f_a g'_{\delta a} A_2(-\kappa_a, \kappa_{\delta a})] + \frac{1}{p} b_1(\rho) [g_a f_{\delta a} A_3(\kappa_a, -\kappa_{\delta a}) + f_a g_{\delta a} A_3(-\kappa_a, \kappa_{\delta a})] + b_2(\rho) [\tilde{g}_a g_{\delta a} A_4(\kappa_a, \kappa_{\delta a}) + \tilde{f}_a f_{\delta a} A_4(-\kappa_a, -\kappa_{\delta a})] + b_3(\rho) [g_a g_{\delta a} A_4(\kappa_a, \kappa_{\delta a}) - f_a f_{\delta a} A_4(-\kappa_a, -\kappa_{\delta a})] \right\}, \quad (47)$$

where $\tilde{g}_{\delta a} = \varepsilon_a g_{\delta a} + p f_{\delta a}$, $\tilde{f}_{\delta a} = \varepsilon_a f_{\delta a} + p g_{\delta a}$, $\tilde{g}_a = \varepsilon_a g_a + p f_a$, $\tilde{f}_a = \varepsilon_a f_a + p g_a$, $g' = dg(p)/dp$ and $f' = df(p)/dp$, the scalar functions $A(\rho)$, $b_i(\rho)$ are given by Eqs. (24), (30)–(32) of Ref. [34] and $A_i(\kappa_1, \kappa_2)$ are the basic angular integrals defined and evaluated in Appendix A.

Note that the expression for $\Delta\sigma_{\text{ver},\text{zee},2}^{(0)}$ is non-symmetric with respect to a and δa , but the result does not change when the two wave functions are interchanged.

4. Double-vertex contribution

The double-vertex correction is defined by Eq. (27). All parts of it are UV finite and thus can be evaluated in coordinate space. We denote the individual terms in the right-hand-side of Eq. (27) by $\delta_i E$ and consider each of them separately,

$$\Delta E_{\text{d.vr}} = \sum_{i=1}^5 \delta_i E. \quad (48)$$

The first term is

$$\delta_1 E \equiv 2 \langle \Lambda \rangle = 2 \frac{i}{2\pi} \int_{-\infty}^{\infty} d\omega \times \sum_{n_1 n_2 n_3} \frac{\langle an_3 | I(\omega) | n_1 a \rangle \langle n_1 | V_{\text{zee}} | n_2 \rangle \langle n_2 | V_{\text{hfs}} | n_3 \rangle}{(\varepsilon - \omega - u \varepsilon_{n_1})(\varepsilon - \omega - u \varepsilon_{n_2})(\varepsilon - \omega - u \varepsilon_{n_3})}. \quad (49)$$

After separating the nuclear variables and integrating over the angles, the contribution to the magnetic shielding is (for $j_a = 1/2$)

$$\delta_1 \sigma = \frac{i\alpha^2}{2\pi} \int_{-\infty}^{\infty} d\omega \sum_{n_1 n_2 n_3} \sum_J X_J^{\text{d.ver}}(\kappa_1, \kappa_2, \kappa_3) \times \frac{R_J(\omega, an_3 n_1 a) R_{n_1 n_2}^{(1)} R_{n_2 n_3}^{(-2)}}{(\varepsilon - \omega - u \varepsilon_{n_1})(\varepsilon - \omega - u \varepsilon_{n_2})(\varepsilon - \omega - u \varepsilon_{n_3})}, \quad (50)$$

where

$$X_J^{\text{d.ver}}(\kappa_1, \kappa_2, \kappa_3) = \frac{(-1)^{J+j_a-j_2}}{2} \times \sum_{j_n=1/2, 3/2} (2j_n+1) \left\{ \begin{matrix} 1 & j_n & j_a \\ J & j_1 & j_2 \end{matrix} \right\} \left\{ \begin{matrix} 1 & j_n & j_a \\ J & j_3 & j_2 \end{matrix} \right\} \times \frac{\kappa_1 + \kappa_2}{\sqrt{3}} C_1(-\kappa_2, \kappa_1) \frac{\kappa_2 + \kappa_3}{\sqrt{3}} C_1(-\kappa_3, \kappa_2). \quad (51)$$

Note that the expression for $\delta_1 \sigma$ is IR divergent when any two or all three of the intermediate states have the same energy as the reference state: $\varepsilon_{n_1} = \varepsilon_{n_2} = \varepsilon_a$, $\varepsilon_{n_2} = \varepsilon_{n_3} = \varepsilon_a$, $\varepsilon_{n_1} = \varepsilon_{n_3} = \varepsilon_a$, $\varepsilon_{n_1} = \varepsilon_{n_2} = \varepsilon_{n_3} = \varepsilon_a$. The IR divergence cancels when all parts of Eq. (27) are added together.

The contribution of the second term to the shielding is

$$\delta_2 \sigma = \frac{\alpha}{2} \langle \tilde{V}_{\text{zee}} \rangle \langle \tilde{V}_{\text{hfs}} \rangle \langle \Sigma'' \rangle = \frac{4}{9} R_{aa}^{(1)} R_{aa}^{(-2)} \times \frac{i\alpha^2}{2\pi} \int_{-\infty}^{\infty} d\omega \sum_{n_1 n_2 n_3} \sum_J \frac{(-1)^{J+j_a-j_1}}{2j_a+1} \delta_{\kappa_1, \kappa_2} \delta_{\kappa_1, \kappa_3} \times \frac{R_J(\omega, an_3 n_1 a) N_{n_1 n_2} N_{n_2 n_3}}{(\varepsilon - \omega - u \varepsilon_{n_1})(\varepsilon - \omega - u \varepsilon_{n_2})(\varepsilon - \omega - u \varepsilon_{n_3})}, \quad (52)$$

where N_{ab} is the normalization integral,

$$N_{ab} = \int_0^\infty dx x^2 (g_a g_b + f_a f_b). \quad (53)$$

The expression for $\delta_2 \sigma$ is IR divergent when $\varepsilon_{n_1} = \varepsilon_{n_2} = \varepsilon_{n_3} = \varepsilon_a$.

The third term is given by

$$\delta_3 \sigma = \frac{1}{3} R_{aa}^{(1)} \frac{i\alpha^2}{2\pi} \int_{-\infty}^{\infty} d\omega \sum_{n_1 n_2 n_3} \times \left[\frac{\sum_J X_J(\kappa_1, \kappa_2) \delta_{\kappa_2, \kappa_3} R_J(\omega, an_3 n_1 a) R_{n_1 n_2}^{(-2)} N_{n_2 n_3}}{(\varepsilon - \omega - u \varepsilon_{n_1})(\varepsilon - \omega - u \varepsilon_{n_2})(\varepsilon - \omega - u \varepsilon_{n_3})} + \frac{\sum_J X_J(\kappa_2, \kappa_3) \delta_{\kappa_1, \kappa_2} R_J(\omega, an_3 n_1 a) N_{n_1 n_2} R_{n_2 n_3}^{(-2)}}{(\varepsilon - \omega - u \varepsilon_{n_1})(\varepsilon - \omega - u \varepsilon_{n_2})(\varepsilon - \omega - u \varepsilon_{n_3})} \right], \quad (54)$$

where

$$X_J(\kappa_1, \kappa_2) = \frac{1}{\sqrt{2}} \left\{ \begin{matrix} j_1 & j_2 & 1 \\ j_a & j_a & J \end{matrix} \right\} \frac{-\kappa_1 - \kappa_2}{\sqrt{3}} C_1(-\kappa_2, \kappa_1). \quad (55)$$

The fourth term $\delta_4 \sigma$ is obtained from $\delta_3 \sigma$ by an obvious substitution $R^{(1)} \leftrightarrow R^{(-2)}$.

The fifth term is given by

$$\delta_5 \sigma = -\sigma^{(0)} \frac{i\alpha}{2\pi} \int_{-\infty}^{\infty} d\omega \frac{\sum_J \frac{(-1)^J}{2j_a+1} R_J(\omega, aaaa)}{(-\omega + i0)^2}. \quad (56)$$

Finally, the total double-vertex contribution is given by the sum of the five terms discussed above,

$$\Delta\sigma_{\text{d.vr}} = \sum_{i=1}^5 \delta_i \sigma. \quad (57)$$

Despite the fact that the individual terms $\delta_i \sigma$ are IR divergent, the sum of them is finite and can be evaluated without any explicit regularization, provided that (i) the integration over the frequency of the virtual photon in the self-energy loop ω is performed after all five terms are added together and (ii) the contour of the ω integration is suitably chosen. One can show that if the ω integration is performed along the contour consisting of the low-energy and high-energy parts, as e.g., in Refs. [30, 31], the integrand becomes regular at $\omega \rightarrow 0$ and, therefore, can be directly evaluated numerically.

The numerical evaluation of the double-vertex correction $\Delta\sigma_{\text{d.vr}}$ was the most time consuming part of our calculation, due to a large number of the partial waves involved and a four-dimensional radial integration in Eq. (50). The radial integration was carried out with help of the numerical approach developed in our calculation of the two-loop self-energy and described in detail in Ref. [29]. Because of numerical cancellations between the five terms in Eq. (57), especially in the region of small values of ω , we took care to treat all five terms exactly in the same way. In particular, the normalization integrals N_{ab} in Eqs. (52) and (54) were evaluated numerically, in order to be consistent with the evaluation of Eq. (50), whereas the corresponding contributions could have been evaluated more easily by taking the derivative of the Dirac-Coulomb Green function.

C. Vacuum polarization correction

Vacuum polarization corrections to the magnetic shielding calculated in the present work are shown in Fig. 2. The diagrams in Fig. 2(a)-(c) come from the insertion of the Uehling potential into the electron line of the leading-order magnetic shielding, whereas the diagram in Fig. 2(d) represents the Uehling potential insertion into the hfs interaction. We note that the diagram with the vacuum polarization insertion into the Zeeman interaction vanishes in the Uehling-potential approximation. In our treatment, we neglect contributions with additional Coulomb interactions in the vacuum-polarization loop (which correspond to the Wichmann-Kroll part of the one-loop vacuum polarization) and the additional diagram of the Wichmann-Kroll type with both hfs and Zeeman interactions attached to the vacuum-polarization loop. We expect that the part accounted for in the present work yields the dominant contribution to the vacuum polarization correction.

The contribution of the diagrams in Fig. 2 (a)-(c) is an analogue of the perturbed-orbital self-energy contribution and is given by a similar expression,

$$\Delta\sigma_{\text{VP},\text{po}} = \alpha \langle a_{1/2} | V_{\text{Ueh}} | \delta^{(2)} a_{1/2} \rangle + \alpha \langle \delta_{\text{hfs}}^{(1)} a_{1/2} | V_{\text{Ueh}} | \delta_{\text{zee}}^{(1)} a_{1/2} \rangle, \quad (58)$$

where V_{Ueh} is the Uehling potential,

$$V_{\text{Ueh}}(r) = -\frac{2\alpha^2 Z}{3mr} \int_0^\infty dr' r' \rho(r') \times [K_0(2m|r-r'|) - K_0(2m|r+r'|)], \quad (59)$$

and

$$K_0(x) = \int_1^\infty dt e^{-xt} \left(\frac{1}{t^3} + \frac{1}{2t^5} \right) \sqrt{t^2 - 1}, \quad (60)$$

and the nuclear-charge density ρ is normalized by the condition $\int d\vec{r} \rho(r) = 1$. We note that this contribution can also be calculated by incorporating the Uehling potential into the Dirac equation and re-evaluating the leading-order magnetic shielding, in this way accounting for the Uehling potential to all orders. We performed calculations in both ways, which ensured that the perturbations of the reference-state wave function $|\delta^{(1)} a\rangle$ and $|\delta^{(2)} a\rangle$ are computed correctly.

The contribution of the diagram in Fig. 2(d) to the magnetic shielding can be expressed as

$$\Delta\sigma_{\text{VP},\text{mag}} = \alpha \sum_{n \neq a} \frac{1}{\varepsilon_a - \varepsilon_n} \times \langle a_{1/2} | \tilde{V}_{\text{zee}} | n_{1/2} \rangle \langle n_{1/2} | \tilde{V}_{\text{VP},\text{mag}} | a_{1/2} \rangle, \quad (61)$$

where

$$\tilde{V}_{\text{VP},\text{mag}}(r) = \tilde{V}_{\text{hfs}}(r) \frac{2\alpha}{3\pi} \int_1^\infty dt \frac{\sqrt{t^2 - 1}}{t^2} \times \left(1 + \frac{1}{2t^2} \right) (1 + 2mrt) e^{-2mrt} \quad (62)$$

is the hfs interaction modified by the vacuum-polarization insertion.

IV. QED CORRECTION FOR SMALL NUCLEAR CHARGES

In the previous section, we calculated the QED corrections to the magnetic shielding without any expansion in the nuclear binding strength parameter $Z\alpha$. Now we turn to the evaluation of this corrections within the expansion in this parameter. We will derive the complete expression for the leading term of the $Z\alpha$ expansion, which enters in the relative order $\delta\sigma/\sigma \sim \alpha(Z\alpha)^2$. The results obtained in this section will be applicable for light hydrogen-like ions, where no all-order calculations were possible because of large numerical cancellation. They will also provide an important cross-check with the all-order calculations described in the previous section.

For the derivation, it is convenient to use the formalism of the non-relativistic quantum electrodynamics (NRQED). In this approach, all QED effects are calculated by an expansion in powers of α and $Z\alpha$ and represented as expectation values of various effective operators on the nonrelativistic reference-state wave function. Let us start with the effective Hamiltonian H_{NRQED} , which includes leading one-loop radiative corrections:

$$H_{\text{NRQED}} = \frac{\vec{\pi}^2}{2m} + eA^0 - \frac{e}{6} \left(\frac{3}{4m^2} + r_E^2 \right) \vec{\nabla} \cdot \vec{E} + \frac{e}{12m} \left(r_E^2 - \frac{3\kappa}{4m^2} \right) \{ \vec{\pi}, \vec{\nabla} \times \vec{B} \} - \frac{e^2}{2} \left(\frac{1}{4m^3} + \alpha_M \right) \vec{B}^2, \quad (63)$$

where $\{ \cdot, \cdot \}$ denotes anticommutator, $\vec{\pi} = \vec{p} - e\vec{A}$. The QED effects in the above Hamiltonian are parameterized in terms of the constants κ , r_E , and α_M , which are interpreted as the electron magnetic moment anomaly, the charge radius and the magnetic polarizability, respectively,

$$\kappa = \frac{\alpha}{2\pi}, \quad (64)$$

$$r_E^2 = \frac{3\kappa}{2m^2} + \frac{2\alpha}{\pi m^2} \left(\ln \frac{m}{2\epsilon} + \frac{11}{24} \right), \quad (65)$$

$$\alpha_M = \frac{4\alpha}{3\pi m^3} \left(\ln \frac{m}{2\epsilon} + \frac{13}{24} \right), \quad (66)$$

where ϵ is the photon momentum cutoff. In the non-QED limit, all QED constants vanish, $r_E^2 = \alpha_M = \kappa = 0$, and the effective Hamiltonian H_{NRQED} turns into the Schrödinger-Pauli Hamiltonian.

The QED constants r_E^2 and α_M depend explicitly on the photon momentum cutoff parameter ϵ . This dependence cancels out with contributions coming from the emission and absorption of virtual photons with the energy smaller than ϵ . The complete expression for any

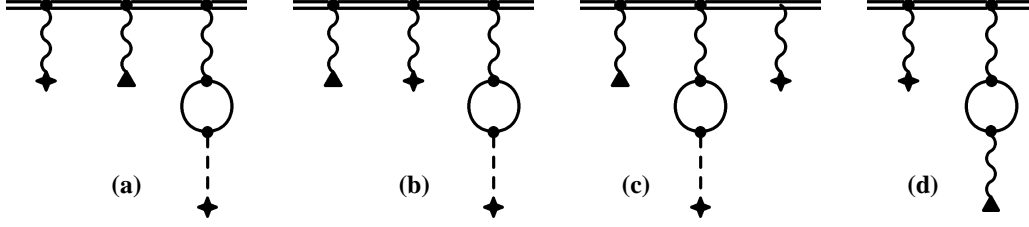


FIG. 2: Vacuum-polarization corrections to the nuclear magnetic shielding calculated in the present work. The double line represents electron propagating in the binding nuclear field, the single line represents the free-electron propagator, the dashed line terminated by a cross represents interaction with the binding Coulomb field, the wave line terminated by a triangle represents the dipole hyperfine interaction with the nucleus, and the wave line terminated by a cross represents the interaction with the external magnetic field.

physical quantity, e.g., the Lamb shift and the shielding constant, does not depend on the artificial photon cutoff parameter.

The above formula for r_E^2 is obtained from the well known expressions for the one-loop radiative corrections to electromagnetic formfactors F_1 and F_2 [40]. The formula for α_M has not appeared in the literature previously. We have derived it by a method similar to that used in Ref. [41] for the electric polarizability, denoted by χ in that work.

We will start with rederiving the known nonrelativistic expression for the shielding constant within our approach. It comes from the \vec{A}^2 term in the electron kinetic energy in Eq. (63). The electromagnetic potential \vec{A} is the sum of the external magnetic potential \vec{A}_E ,

$$\vec{A}_E = \frac{1}{2} \vec{B} \times \vec{r}, \quad (67)$$

and the potential induced by the nuclear magnetic moment,

$$\vec{A}_I = \frac{1}{4\pi} \vec{\mu} \times \frac{\vec{r}}{r^3}. \quad (68)$$

The corresponding energy shift is

$$\begin{aligned} \delta E &= \frac{e^2}{2m} \langle \vec{A}^2 \rangle = \frac{e^2}{m} \langle \vec{A}_E \cdot \vec{A}_I \rangle \\ &= \frac{\alpha}{2m} \left\langle \left(\vec{B} \times \vec{r} \right) \cdot \left(\vec{\mu} \times \frac{\vec{r}}{r^3} \right) \right\rangle, \end{aligned} \quad (69)$$

where matrix elements are calculated with the nonrelativistic wave function. The shielding constant σ is obtained from the energy shift δE by $\delta E = \sigma \vec{\mu} \cdot \vec{B}$. For the ground ($L = 0$) hydrogenic state, the nonrelativistic results is

$$\sigma = \frac{\alpha}{3m} \left\langle \frac{1}{r} \right\rangle. \quad (70)$$

Before considering the QED effects to the shielding constant, it is convenient to first recalculate the leading

QED correction to the energy levels. The total contribution is split into two parts induced by the virtual photons of low (L) and high (H) energy,

$$\delta E_{\text{Lamb}} = \delta E_L + \delta E_H. \quad (71)$$

The high-energy part is the expectation value of the $\vec{\nabla} \cdot \vec{E}$ term in the effective Hamiltonian in Eq. (63)

$$\begin{aligned} \delta E_H &= \left\langle -\frac{e}{6} r_E^2 \vec{\nabla} \cdot \vec{E} \right\rangle = \frac{2}{3} \frac{(Z\alpha)^4}{n^3} r_E^2 \delta_{l0} \\ &= \frac{\alpha}{\pi} \frac{(Z\alpha)^4}{n^3} \left(\frac{4}{3} \ln \frac{m}{2\epsilon} + \frac{10}{9} \right) \delta_{l0}, \end{aligned} \quad (72)$$

where $\vec{E} = -\vec{\nabla} A^0$ and $A^0 = -Ze/(4\pi r)$. The vacuum polarization can be incorporated in the above expression by adding $-2\alpha/(5\pi m^2)$ to r_E^2 in Eq. (65). The low-energy part δE_L is induced by the emission and the absorption of the virtual photons of low ($k < \epsilon$) energy,

$$\begin{aligned} \delta E_L &= e^2 \int_0^\epsilon \frac{d^3 k}{(2\pi)^3 2k} \left(\delta^{ij} - \frac{k^i k^j}{k^2} \right) \left\langle \frac{p^i}{m} \frac{1}{E - H - k} \frac{p^j}{m} \right\rangle \\ &= \frac{2\alpha}{3\pi} \left\langle \frac{\vec{p}}{m} (H - E) \left\{ \ln \left[\frac{2\epsilon}{m(Z\alpha)^2} \right] - \ln \left[\frac{2(H - E)}{m(Z\alpha)^2} \right] \right\} \frac{\vec{p}}{m} \right\rangle. \end{aligned} \quad (73)$$

The terms containing $\ln \epsilon$ cancel out in the sum of the low- and high-energy parts, as expected. The total leading-order Lamb shift contribution is

$$\begin{aligned} \delta E_{\text{Lamb}} &= \frac{\alpha}{\pi} \frac{(Z\alpha)^4}{n^3} \left\{ \frac{4}{3} \ln[(Z\alpha)^{-2}] \delta_{l0} \right. \\ &\quad \left. + \left(\frac{10}{9} - \frac{4}{15} \right) \delta_{l0} - \frac{4}{3} \ln k_0(n, l) \right\}, \end{aligned} \quad (74)$$

where $\ln k_0(n, l)$ is the Bethe logarithm,

$$\ln k_0(n, l) = \frac{n^3}{2m^3 (Z\alpha)^4} \left\langle \vec{p} (H - E) \ln \left[\frac{2(H - E)}{m(Z\alpha)^2} \right] \vec{p} \right\rangle. \quad (75)$$

We now turn to the calculation of the QED correction to the magnetic shielding, which is performed similarly

to that for the Lamb shift. The total contribution is split into the low and the high-energy parts:

$$\delta E = \delta E_L + \delta E_H, \quad (76)$$

where

$$\delta E_L = e^2 \int_0^\epsilon \frac{d^3 k}{(2\pi)^3 2k} \left(\delta^{ij} - \frac{k^i k^j}{k^2} \right) \left\langle \frac{\pi^i}{m} \frac{1}{E-H-k} \frac{\pi^j}{m} \right\rangle, \quad (77)$$

and

$$\begin{aligned} \delta E_H = & -2 \left\langle \frac{e}{6} r_E^2 \vec{\nabla} \cdot \vec{E} \frac{1}{(E-H)'} \frac{\vec{A}^2}{2m} \right\rangle \\ & + \left\langle \frac{e}{12m} \left(r_E^2 - \frac{3\kappa}{4m^2} \right) \{ \vec{\pi}, \vec{\nabla} \times \vec{B} \} \right\rangle - \left\langle \frac{e^2}{2} \alpha_M \vec{B}^2 \right\rangle. \end{aligned} \quad (78)$$

The high-energy part can be conveniently rewritten in the form

$$\begin{aligned} \delta E_H = & \frac{1}{9} Z \alpha^2 r_E^2 \left\langle \frac{1}{r} \frac{1}{(E-H)'} 4\pi \delta^3(r) \right\rangle \vec{\mu} \cdot \vec{B} \\ & - \frac{2\pi\alpha}{3m} \left(r_E^2 - \frac{3\kappa}{4m^2} \right) \langle \vec{A}_E \cdot \vec{\nabla} \times \vec{B}_I \rangle \\ & - 4\pi\alpha\alpha_M \langle \vec{B} \cdot \vec{B}_I \rangle. \end{aligned} \quad (79)$$

In the low-energy part, we separate out $\ln \epsilon$ and then perform an expansion in the magnetic fields,

$$\delta E_L = \delta E_{LA} + \delta E_{LB}, \quad (80)$$

$$\delta E_{LA} = -\frac{2\alpha}{3\pi} \left\langle \frac{\vec{\pi}}{m} (H-E) \ln \frac{2(H-E)}{m(Z\alpha)^2} \frac{\vec{\pi}}{m} \right\rangle, \quad (81)$$

$$\delta E_{LB} = \frac{2\alpha}{3\pi} \left\langle \frac{\vec{\pi}}{m} (H-E) \frac{\vec{\pi}}{m} \right\rangle \ln \frac{2\epsilon}{m(Z\alpha)^2}. \quad (82)$$

Using the identity

$$\begin{aligned} 2 \left\langle \frac{\vec{\pi}}{m} (H-E) \frac{\vec{\pi}}{m} \right\rangle &= \left\langle \left[\frac{\vec{\pi}}{m}, \left[H-E, \frac{\vec{\pi}}{m} \right] \right] \right\rangle \\ &= \left\langle 4\pi Z \alpha \delta^3(r) + \frac{e}{2m^3} \{ \vec{\pi}, \vec{\nabla} \times \vec{B} \} + \frac{2e^2}{m^3} B^2 \right\rangle, \end{aligned} \quad (83)$$

we transform δE_{LB} to the form

$$\begin{aligned} \delta E_{LB} = & \frac{\alpha}{3\pi} \ln \left[\frac{2\epsilon}{m(Z\alpha)^2} \right] \\ & \left[2 \left\langle \frac{\alpha}{3r} \frac{1}{(E-H)'} 4\pi Z \alpha \delta^3(r) \right\rangle \vec{\mu} \cdot \vec{B} \right. \\ & \left. - 4\pi\alpha \langle \vec{A}_E \cdot \vec{\nabla} \times \vec{B}_I \rangle + 16\pi\alpha \langle \vec{B} \cdot \vec{B}_I \rangle \right]. \end{aligned} \quad (84)$$

The artificial parameter $\ln \epsilon$ cancels out in the sum $\delta E_{LB} + \delta E_H$ separately for each type of the matrix elements,

$$\begin{aligned} \delta E_{LB} + \delta E_H = & \frac{2}{9} \frac{\alpha^2}{\pi} Z \alpha \\ & \times \left[\ln(Z\alpha)^{-2} + \frac{5}{6} - \frac{1}{5} \right] \vec{\mu} \cdot \vec{B} \left\langle 4\pi \delta^3(r) \frac{1}{(E-H)'} \frac{1}{r} \right\rangle \\ & - \frac{4}{3} \alpha^2 \left[\ln(Z\alpha)^{-2} + \frac{31}{48} - \frac{1}{5} \right] \langle \vec{A}_E \cdot \vec{\nabla} \times \vec{B}_I \rangle \\ & + \frac{16}{3} \alpha^2 \left[\ln(Z\alpha)^{-2} - \frac{13}{24} \right] \langle \vec{B} \cdot \vec{B}_I \rangle. \end{aligned} \quad (85)$$

Using the following results for the matrix elements with nS states

$$\left\langle 4\pi \delta^3(r) \frac{1}{(E-H)'} \frac{1}{r} \right\rangle = -\frac{6(Z\alpha)^2}{n^3}, \quad (86)$$

$$\langle \vec{A}_E \cdot \vec{\nabla} \times \vec{B}_I \rangle = \frac{(Z\alpha)^3}{\pi n^3} \vec{\mu} \cdot \vec{B}, \quad (87)$$

$$\langle \vec{B} \cdot \vec{B}_I \rangle = \frac{2}{3\pi} \frac{(Z\alpha)^3}{n^3} \vec{\mu} \cdot \vec{B}, \quad (88)$$

we obtain

$$\delta E_{LB} + \delta E_H = \frac{8\alpha^2}{9\pi} \frac{(Z\alpha)^3}{n^3} \left[\ln(Z\alpha)^{-2} - \frac{421}{96} + \frac{3}{5} \right] \vec{\mu} \cdot \vec{B}. \quad (89)$$

The calculation of the remaining low-energy contribution δE_{LA} is slightly more complicated. We first return to the integral form of δE_L , derive an expression for δE_{LA} , and then drop all terms with $\ln \epsilon$, as they are already accounted for by δE_{LB} . The integral form of δE_L is

$$\delta E_L = \frac{2\alpha}{3\pi} \int_0^\epsilon k dk \left\langle \frac{\vec{\pi}}{m} \frac{1}{E-H-k} \frac{\vec{\pi}}{m} \right\rangle. \quad (90)$$

It can be rewritten, using the identity $\vec{\pi} = -im[\vec{r}, H-E]$, in the form

$$\delta E_L = \frac{2\alpha}{3\pi} \int_0^\epsilon k^3 dk \left\langle \vec{r} \frac{1}{E-H-k} \vec{r} \right\rangle. \quad (91)$$

All terms with positive powers of ϵ are discarded, since one assumes that the limit $\epsilon \rightarrow 0$ is taken after the expansion in α is done. We shall now expand the integrand in Eq. (91) in the magnetic fields. The Hamiltonian H is

$$H = H_0 + \frac{\alpha}{3r} \vec{\mu} \cdot \vec{B} - \frac{e}{2m} \vec{L} \cdot \vec{B} - \frac{e}{4\pi m r^3} \vec{L} \cdot \vec{\mu}, \quad (92)$$

where $H_0 = p^2/(2m) - Z\alpha/r$. The first term with \vec{B} in Eq. (92) can be absorbed into $Z' = Z - \vec{\mu} \cdot \vec{B}/3$. So, the correction due to this term is

$$\begin{aligned} \delta E_{L1} = & \frac{4\alpha}{3\pi} (Z'\alpha)^4 \left\{ \ln \left[\frac{2\epsilon}{m(Z'\alpha)^2} \right] - \ln k_0 \right\} \\ = & \frac{16\alpha^2}{9\pi} \frac{(Z\alpha)^3}{n^3} \vec{\mu} \cdot \vec{B} \left\{ \ln k_0 + \frac{1}{2} - \ln \left[\frac{2\epsilon}{m(Z\alpha)^2} \right] \right\}. \end{aligned} \quad (93)$$

The correction due to the two last terms in Eq. (92) is

$$\begin{aligned}
\delta E_{L2} &= \frac{2\alpha^2}{3\pi m^2} \int_0^\epsilon dk k^3 \left\langle \vec{r} \frac{1}{E-H-k} \vec{L} \cdot \vec{B} \frac{1}{E-H-k} \frac{\vec{\mu} \cdot \vec{L}}{r^3} \frac{1}{E-H-k} \vec{r} \right\rangle \\
&= \frac{2\alpha^2}{9\pi} \vec{\mu} \cdot \vec{B} \int_0^\epsilon dk k^3 \frac{d}{dk} \left\langle \vec{r} \frac{1}{E-H-k} \frac{1}{r^3} \frac{1}{E-H-k} \vec{r} \right\rangle.
\end{aligned} \tag{94}$$

Integrating by parts and using the results and the notation of $\ln k_3$ from Ref. [12]

$$\begin{aligned}
&\int_0^\epsilon dk k^2 \left\langle \vec{r} \frac{1}{E-H-k} \frac{1}{r^3} \frac{1}{E-H-k} \vec{r} \right\rangle \\
&= \epsilon \left\langle \frac{1}{r} \right\rangle - \frac{4(Z\alpha)^3}{n^3} \left\{ \ln \left[\frac{2\epsilon}{m(Z\alpha)^2} \right] - \ln k_3 \right\},
\end{aligned} \tag{95}$$

we obtain

$$\delta E_{L2} = \frac{8\alpha^2}{3\pi m^2} \frac{(Z\alpha)^3}{n^3} \vec{\mu} \cdot \vec{B} \left\{ \ln \left[\frac{2\epsilon}{m(Z\alpha)^2} \right] - \ln k_3 - \frac{1}{3} \right\}. \tag{96}$$

The sum of these two contributions $\delta E_{LA} = \delta E_{L1} + \delta E_{L2}$, after dropping the $\ln \epsilon$ terms, is

$$\delta E_{LA} = \frac{8\alpha^2}{9\pi} \frac{(Z\alpha)^3}{n^3} \vec{\mu} \cdot \vec{B} (2 \ln k_0 - 3 \ln k_3). \tag{97}$$

Finally, the total correction to energy is

$$\delta E = \delta E_{LA} + \delta E_{LB} + \delta E_H. \tag{98}$$

Expressing the energy shift in terms of the shielding constant ($\delta E = \delta \sigma \vec{\mu} \cdot \vec{B}$), we obtain the complete result for the leading QED correction to the nuclear magnetic shielding in hydrogen-like ions, valid for the nS states,

$$\begin{aligned}
\delta \sigma &= \frac{8\alpha^2}{9\pi} \frac{(Z\alpha)^3}{n^3} \\
&\times \left\{ \ln[(Z\alpha)^{-2}] + 2 \ln k_0(n) - 3 \ln k_3(n) - \frac{421}{96} + \frac{3}{5} \right\}.
\end{aligned} \tag{99}$$

$$\tag{100}$$

The term of $3/5$ in the brackets is the contribution of the vacuum polarization. The numerical results for the Bethe logarithm $\ln k_0$ and the $1/r^3$ Bethe-logarithm-type correction $\ln k_3$ [12] for the $1s$ state are

$$\ln k_0(1s) = 2.984128556, \tag{101}$$

$$\ln k_3(1s) = 3.272806545. \tag{102}$$

We note that the numerical value of the constant term in Eq. (100), -7.63558 , is comparable in magnitude but of the opposite sign to the logarithmic term at $Z = 1$, $\ln \alpha^{-2} = 9.84049$. This entails a significant numerical cancellation between these two terms for hydrogen and light hydrogen-like ions. As a result, the total QED correction turns out to be much smaller in magnitude than could be anticipated from the leading logarithm alone.

V. OTHER CORRECTIONS

A. Bohr-Weisskopf correction

We now turn to the effect induced by the spatial distribution of the nuclear magnetic moment, also known as the Bohr-Weisskopf (BW) correction. Our treatment of the BW effect is based on the effective single-particle (SP) model of the nuclear magnetic moment. Within this model, the magnetic moment is assumed to be induced by the odd nucleon (proton, when Z and A are odd and neutron, when Z is even and A is odd) with an effective g -factor, which is adjusted to yield the experimental value of the nuclear magnetic moment. The treatment of the magnetization distribution effect on hfs within the SP model was originally developed in Refs. [42, 43] and later in Ref. [44]. Our present treatment closely follows the procedure described in Refs. [44–46].

The wave function of the odd nucleon is assumed to satisfy the Schrödinger equation with the central potential of Woods-Saxon form and the spin-orbital term included (see, e.g., Ref. [47])

$$V(\vec{r}) = -V_0 \mathcal{F}(r) + \frac{1}{m_p} \phi_{so}(r) \vec{l} \cdot \vec{\sigma} + V_C(r), \tag{103}$$

where

$$\phi_{so}(r) = \frac{V_{so}}{4m_p r} \frac{d\mathcal{F}(r)}{dr}, \tag{104}$$

$$\mathcal{F}(r) = \left[1 + \exp \left(\frac{r-R}{a} \right) \right]^{-1}, \tag{105}$$

and V_C is the Coulomb part of the interaction (absent for neutron), with the uniform distribution of the charge $(Z-1)$ over the nuclear sphere. The parameters V_0 , V_{so} , R , and a were taken from Refs. [47, 48].

The nuclear magnetic moment can be evaluated within the SP model to yield [45]

$$\frac{\mu}{\mu_N} = \begin{cases} \frac{1}{2} g_S + \left[I - \frac{1}{2} + \frac{2I+1}{4(I+1)} \langle \phi_{so} r^2 \rangle \right] g_L, & \text{for } I = L + \frac{1}{2}, \\ -\frac{I}{2(I+1)} g_S + \left[\frac{I(2I+3)}{2(I+1)} - \frac{2I+1}{4(I+1)} \langle \phi_{so} r^2 \rangle \right] g_L, & \text{for } I = L - \frac{1}{2}, \end{cases} \tag{106}$$

where I and L are the total and the orbital angular momentum of the nucleus, respectively, g_L is the g factor associated with the orbital motion of the nucleon ($g_L = 1$ for proton and $g_L = 0$ for neutron) and g_S is the effective nucleon g factor, determined by the condition that Eq. (106) yields the experimental value of the magnetic

moment.

It was demonstrated in Ref. [45] that, within the SP model, the BW effect can be accounted for by adding a multiplicative magnetization-distribution function $F(r)$ to the standard point-dipole hfs interaction. The distribution function is given by [46]

$$F(r) = \frac{\mu_N}{\mu} \int_0^r dr' r'^2 |u(r')|^2 \left[\frac{1}{2} g_S + \left(I - \frac{1}{2} + \frac{2I+1}{4(I+1)} r^2 \phi_{so}(r) \right) g_L \right] + \frac{\mu_N}{\mu} \int_r^\infty dr' r'^2 |u(r')|^2 \frac{r^3}{r'^3} \left[-\frac{2I-1}{8(I+1)} g_S + \left(I - \frac{1}{2} + \frac{2I+1}{4(I+1)} r^2 \phi_{so}(r) \right) g_L \right], \quad (107)$$

for $I = L + 1/2$ and

$$F(r) = \frac{\mu_N}{\mu} \int_0^r dr' r'^2 |u(r')|^2 \left[-\frac{I}{2(I+1)} g_S + \left(\frac{I(2I+3)}{2(I+1)} - \frac{2I+1}{4(I+1)} r^2 \phi_{so}(r) \right) g_L \right] + \frac{\mu_N}{\mu} \int_r^\infty dr' r'^2 |u(r')|^2 \frac{r^3}{r'^3} \left[\frac{2I+3}{8(I+1)} g_S + \left(\frac{I(2I+3)}{2(I+1)} - \frac{2I+1}{4(I+1)} r^2 \phi_{so}(r) \right) g_L \right], \quad (108)$$

for $I = L - 1/2$. In the above formulas, $u(r)$ is the wave function of the odd nucleon. It can easily be seen that $F(r) = 1$ outside the nucleus.

B. Recoil and quadrupole corrections

The recoil correction to the magnetic shielding was obtained in Ref. [18] in the nonrelativistic approximation,

$$\delta\sigma_{\text{rec}} = -\frac{\alpha Z\alpha}{3} \frac{m}{M} \left(1 + \frac{g_N - 1}{g_N} \right), \quad (109)$$

where M is the nuclear mass and

$$g_N = \frac{M}{Zm_p} \frac{\mu}{\mu_N I}. \quad (110)$$

The electric-quadrupole correction to the magnetic shielding is

$$\delta\sigma_Q = -\frac{3Q}{2I(2I-1)} \frac{\delta g_Q}{(m/m_p)g_I}, \quad (111)$$

where Q is the quadrupole moment of the nucleus and δg_Q is the quadrupole correction to the g factor calculated in Ref. [17],

$$\begin{aligned} \delta g_Q &= \alpha (Z\alpha)^3 \frac{12 [35 + 20\gamma - 32(Z\alpha)^2]}{135 \gamma (1 + \gamma)^2 [15 - 16(Z\alpha)^2]} \\ &= \alpha (Z\alpha)^3 \left[\frac{11}{135} + \frac{43}{405} (Z\alpha)^2 + \dots \right]. \end{aligned} \quad (112)$$

VI. RESULTS AND DISCUSSION

Numerical results for the self-energy correction to the nuclear magnetic shielding can be conveniently parameterized in terms of the dimensionless function $D_{\text{SE}}(Z\alpha)$ defined as

$$\Delta\sigma_{\text{SE}} = \alpha^2 (Z\alpha)^3 D_{\text{SE}}(Z\alpha). \quad (113)$$

Our numerical all-order (in $Z\alpha$) results for the self-energy correction to the magnetic shielding are summarized in Table I. We note significant numerical cancellation between the individual contributions, which is particularly strong for low values of Z . The fact that the resulting sum is a smooth function of Z and demonstrates the expected Z scaling serves as a consistency check of our calculations. Besides of numerical cancellation, the additional complication arising in the low- Z region is that the convergence of the partial-wave expansions becomes slower when Z decreases. Because of these two complications, the accuracy of our results worsens for smaller values of Z and no all-order results were obtained for $Z < 10$.

The all-order numerical results can be compared with the $Z\alpha$ -expansion results obtained in Sec. IV. As follows from Eq. (100), the $Z\alpha$ expansion of the function D_{SE} for the $1s$ state reads

$$D_{\text{SE}}(Z\alpha) = \frac{8}{9\pi} \left[\ln(Z\alpha)^{-2} - 8.235\,579 + O(Z\alpha) \right], \quad (114)$$

where $O(Z\alpha)$ denotes the higher-order terms. In Fig. 3, the numerical all-order results for the function D_{SE} are

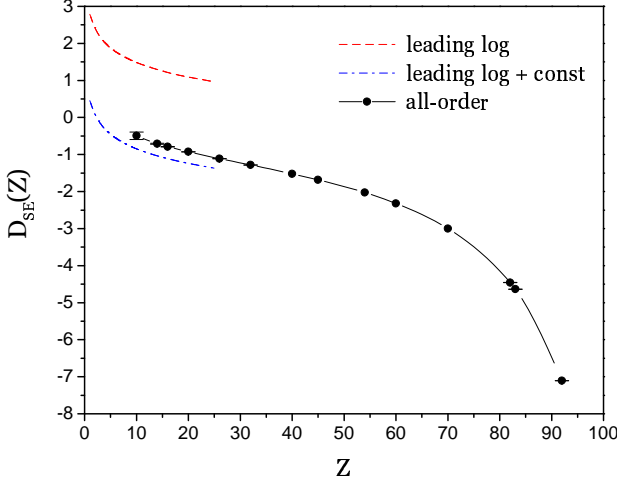


FIG. 3: (Color online) Self-energy correction to the nuclear magnetic shielding.

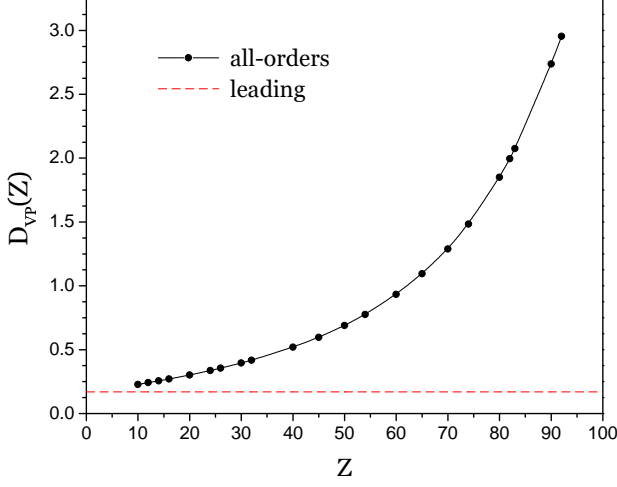


FIG. 4: (Color online) Vacuum-polarization correction to the nuclear magnetic shielding.

plotted together with the contribution of the leading logarithmic term in Eq. (114) (dashed line, red) and the contribution of both terms in Eq. (114) (dashed-dot line, blue). We observe that the leading logarithm alone gives a large contribution that disagrees strongly with the all-order results. However, when the constant term is added, the total $Z\alpha$ -expansion contribution shrinks significantly and even changes its sign for $Z > 3$. Only after the constant term is accounted for, we observe reasonable agreement between the all-order and $Z\alpha$ expansion results.

The vacuum-polarization correction to the nuclear magnetic shielding is parameterized as

$$\Delta\sigma_{VP} = \alpha^2 (Z\alpha)^3 D_{VP}(Z\alpha). \quad (115)$$

Our numerical results for the vacuum-polarization cor-

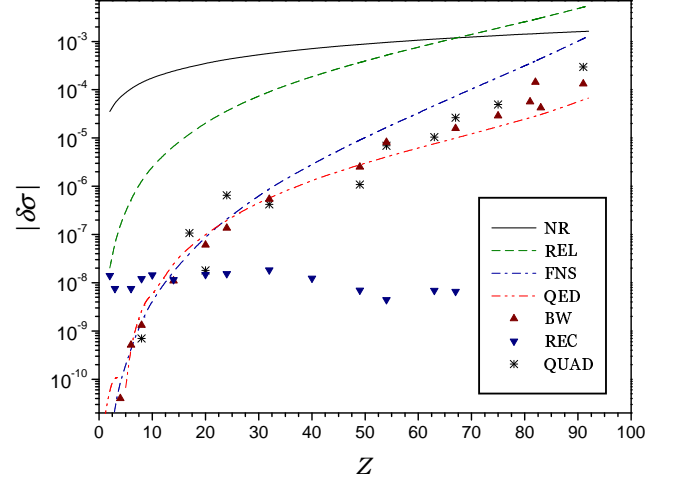


FIG. 5: (Color online) Individual contributions to the nuclear shielding. “NR” is the nonrelativistic contribution, “REL” is the relativistic point-nucleus contribution, “FNS” is the finite nuclear size correction, “QED” is the QED correction, “BW” is the Bohr-Weisskopf correction, “REC” is the recoil correction, and “QUAD” is the electric quadrupole correction. Note that the QED correction changes its sign between $Z = 4$ and 5.

rection are presented in Table II. The calculation was performed for the extended nucleus and the Uehling potential was included to all orders. Note that our present treatment is not complete, as the Wichmann-Kroll part of the correction is still missing. We estimate the uncertainty due to omitted terms to be within 30% of the calculated contribution.

The $Z\alpha$ expansion of the function D_{VP} reads

$$D_{VP}(Z\alpha) = \frac{8}{9\pi n^3} \frac{3}{5} \delta_{l,0} + O(Z\alpha), \quad (116)$$

where the Kronecker symbol $\delta_{l,0}$ indicates that the correction vanishes for the reference states with $l > 0$. Comparison of the all-order numerical results with the leading term of the $Z\alpha$ expansion is given in Fig. 4. It is remarkable that the all-order results grow fast when Z is increased and eventually become more than an order of magnitude larger than the leading-order result. In the high- Z region, the self-energy and vacuum-polarization corrections are (as usual) of the opposite sign, the self energy being about twice larger than the vacuum polarization. In the low- Z region, however, the self-energy correction changes its sign and the total QED contribution becomes positive for very light ions.

The summary of our calculations of the nuclear magnetic shielding constant σ for several hydrogen-like ions is given in Table III. The first line of the table presents results for the leading-order nuclear shielding, including the finite nuclear size effect. The leading-order contribution was calculated using the Fermi model for the nuclear charge distribution and the point-dipole approximation for the interaction with the nuclear magnetic mo-

ment. The nuclear charge radii were taken from Ref. [49]. The results are in good agreement with those reported in Ref. [17]. The QED correction presented in the second line of Table III is the sum of the all-order results for the self energy and the vacuum polarization. Its error comes from the numerical uncertainty of the self-energy part and the estimate of uncalculated vacuum-polarization diagrams. Since there were no all-order calculations performed for oxygen, we used an extrapolation of our all-order results (taking into account the derived values of the $Z\alpha$ expansion coefficients).

The Bohr-Weisskopf correction, presented in the third line of Table III, was calculated by reevaluating the leading-order contribution with the point-dipole hfs interaction modified by the extended-distribution function $F(r)$ given by Eqs. (107) and (108). Because the effective single-particle model of the nuclear magnetic moment is (of course) a rather crude approximation, we estimate the uncertainty of the Bohr-Weisskopf correction to be 30%, which is consistent with previous estimates of the uncertainty of this effect [45]. This uncertainty includes also the error due to the nuclear polarization effect, which is not considered in the present work.

The quadrupole and the recoil corrections, given in the fourth and fifth lines of Table III, respectively, were evaluated according to Eqs. (111) and (109). The error of the quadrupole correction comes from the nuclear quadrupole moments. The magnetic dipole and electric quadrupole moments of nuclei were taken from Refs. [50, 51].

The Z dependence of individual contributions to the magnetic shielding constant σ is shown in Fig. 5. The leading-order contribution is separated into three parts, the point-nucleus nonrelativistic part (solid line, black), the point-nucleus relativistic part (dashed line, green), and the finite nuclear size correction (dashed-dotted line, blue). We observe that the finite nuclear size correction, as well as the other effects calculated in this work, become increasingly important in the region of large nuclear charges. The only exception is the nuclear recoil correction. It practically does not depend on the nuclear charge number Z , since the linear Z scaling in Eq. (109) is compensated by the increase of the nuclear mass M with Z . As a consequence, the recoil effect is completely negligible for high- and medium- Z ions, but turns into one of the dominant corrections for $Z < 10$.

For most ions, the uncertainty of the theoretical prediction is roughly 30% of the Bohr-Weisskopf effect; it can be immediately estimated from Fig. 5. For very light ions, however, there is an additional uncertainty due to the unknown relativistic recoil effect. Its contribution can be estimated by multiplying the nonrelativistic recoil correction plotted on Fig. 5 by the factor of $(Z\alpha)^2$. We observe that for very light ions, the relativistic recoil is the dominant source of error in theoretical predictions.

VII. CONCLUSION

In this work we have performed an *ab initio* calculation of the nuclear magnetic shielding in hydrogen-like ions with inclusion of relativistic, nuclear, and QED effects. The uncertainty of our theoretical predictions for the nuclear magnetic shielding constant defines [according to Eq. (8)] the precision to which the nuclear magnetic dipole moments can be determined from experiments on the g -factors of hydrogen-like ions. It can be concluded from Table III and Fig. 5 that the present theory permits determination of nuclear magnetic moments with fractional accuracy ranging from 10^{-9} in the case of $^{17}\text{O}^{7+}$ to 10^{-5} for $^{209}\text{Bi}^{82+}$.

For most hydrogen-like ions, the dominant source of error in the theoretical predictions is the Bohr-Weisskopf effect. Since this effect cannot be accurately calculated at present, we conclude that the theory of the nuclear magnetic shielding has reached the point where the uncertainty due to nuclear-structure effects impedes further progress. For very light ions, however, the dominant theoretical error comes from the unknown relativistic recoil effect, whose calculation might be a subject of future work.

Acknowledgement

Stimulating discussions with K. Blaum and G. Werth are gratefully acknowledged. V. A. Y. and Z. H. were supported by the Alliance Program of the Helmholtz Association (HA216/EMMI). K.P. acknowledges support by NIST Precision Measurement Grant PMG 60NANB7D6153.

Appendix A: Angular integrals

Throughout this work, we repeatedly used the following result for the matrix element of the hfs and Zeeman interaction

$$\begin{aligned} \langle \kappa_1 \mu_1 | \frac{(\hat{\vec{r}} \times \vec{\alpha})_q}{r^a} | \kappa_2 \mu_2 \rangle &= (-1)^{j_2 + \mu_2} \\ &\times C_{j_2 - \mu_2, j_1 \mu_1}^{1q} P^{(-a)}(n_1, n_2), \end{aligned} \quad (\text{A1})$$

where $\hat{\vec{r}} = \vec{r}/|\vec{r}|$, $C_{j_1 m_1, j_2 m_2}^{j m}$ is the Clebsch-Gordan coefficient, and

$$P^{(\alpha)}(n_1, n_2) = \frac{-\kappa_1 - \kappa_2}{\sqrt{3}} C_1(-\kappa_2, \kappa_1) R_{n_1 n_2}^{(\alpha)}. \quad (\text{A2})$$

The radial integral $R^{(\alpha)}$ is defined by Eq. (16) and the angular coefficient $C_1(\kappa_a, \kappa_b)$ is the reduced matrix element of the normalized spherical harmonics, see, e.g., Eq. (C10) of Ref. [28]. An important particular case is

TABLE I: Individual contributions to the self-energy correction to the nuclear magnetic shielding, for the point nucleus, in terms of the function D_{SE} defined by Eq. (113).

Z	po	vr,hfs	vr,zee	d.ver	der	total
10	-9.584	6.095	9.180	-49.722	43.523	-0.508 (100)
14	-4.741	1.711	4.321	-21.048	19.047	-0.710 (15)
16	-3.571	0.705	3.140	-14.718	13.655	-0.789 (9)
20	-2.217	-0.405	1.761	-7.848	7.782	-0.927 (4)
26	-1.277	-1.115	0.772	-3.473	3.983	-1.110 (2)
32	-0.858	-1.407	0.292	-1.644	2.333	-1.283 (1)
40	-0.624	-1.580	-0.043	-0.586	1.315	-1.519 (1)
45	-0.575	-1.643	-0.171	-0.267	0.975	-1.681
54	-0.595	-1.744	-0.335	0.023	0.622	-2.029
60	-0.672	-1.825	-0.423	0.112	0.487	-2.321
70	-0.929	-2.028	-0.571	0.175	0.355	-2.999
82	-1.612	-2.508	-0.812	0.191	0.284	-4.457 (2)
83	-1.701	-2.569	-0.839	0.192	0.281	-4.636 (1)
92	-3.011	-3.400	-1.174	0.198	0.280	-7.107 (2)

TABLE II: Vacuum-polarization correction to the magnetic shielding, for the extended nucleus, in terms of the function D_{VP} defined by Eq. (115).

Z	po	mag	total
10	0.118	0.110	0.228
14	0.135	0.121	0.256
16	0.144	0.126	0.271
20	0.164	0.137	0.302
26	0.200	0.155	0.355
32	0.242	0.175	0.417
40	0.314	0.206	0.520
45	0.369	0.228	0.597
54	0.500	0.275	0.775
60	0.618	0.315	0.933
70	0.891	0.398	1.289
82	1.449	0.546	1.996
83	1.512	0.562	2.074
92	2.227	0.727	2.954

$\kappa_1 = \kappa_2 = -1$ and $\mu_1 = \mu_2 = 1/2$, in which case the above formulas reduce to

$$\langle -1 \ 1/2 | \frac{(\hat{\vec{r}} \times \vec{\alpha})_0}{r^a} | -1 \ 1/2 \rangle = -\frac{2}{3} R_{ab}^{(-a)}. \quad (\text{A3})$$

The basic angular integrals K_i needed for the evaluation of the hfs vertex contribution are defined by

$$\frac{3i}{4\pi} \int d\hat{p}_1 d\hat{p}_2 F(\xi) \chi_{\kappa_a 1/2}^\dagger(\hat{p}_1) [\hat{p}_1 \times \vec{\sigma}]_0 \chi_{\kappa_b 1/2}(\hat{p}_2) = \int_{-1}^1 d\xi F(\xi) K_1(\kappa_a, \kappa_b), \quad (\text{A4a})$$

$$\frac{3i}{4\pi} \int d\hat{p}_1 d\hat{p}_2 F(\xi) \chi_{\kappa_a 1/2}^\dagger(\hat{p}_1) [\hat{p}_2 \times \vec{\sigma}]_0 \chi_{\kappa_b 1/2}(\hat{p}_2) = \int_{-1}^1 d\xi F(\xi) K'_1(\kappa_a, \kappa_b), \quad (\text{A4b})$$

$$\frac{3i}{4\pi} \int d\hat{p}_1 d\hat{p}_2 F(\xi) \chi_{\kappa_a 1/2}^\dagger(\hat{p}_1) [\hat{p}_1 \times \hat{p}_2]_0 \chi_{\kappa_b 1/2}(\hat{p}_2) = \int_{-1}^1 d\xi F(\xi) K_2(\kappa_a, \kappa_b), \quad (\text{A4c})$$

where $F(\xi)$ is an arbitrary function and $\xi = \hat{p}_1 \cdot \hat{p}_2$. The integrals over all angles except for ξ in the above equations are evaluated analytically, as described in Appendix of Ref. [33]. The results relevant for this work are

$$\begin{aligned} K_1(-1, 1) &= -\xi, \quad K_1(1, -1) = 1, & K_1(-1, -2) &= -\frac{\xi}{\sqrt{2}}, \quad K_1(1, 2) = \frac{-1+3\xi^2}{2\sqrt{2}}, \\ K'_1(-1, 1) &= -1, \quad K'_1(1, -1) = \xi, & K'_1(-1, -2) &= -\frac{1}{\sqrt{2}}, \quad K'_1(1, 2) = \frac{\xi}{\sqrt{2}}, \\ K_2(-1, -1) &= 0, \quad K_2(1, 1) = \frac{-1+\xi^2}{2}, & K_2(-1, 2) &= 0, \quad K_2(1, -2) = \frac{-1+\xi^2}{2\sqrt{2}}. \end{aligned} \quad (\text{A5})$$

TABLE III: Individual contributions to the shielding constant $\sigma \times 10^6$ for selected hydrogen-like ions.

	$^{17}\text{O}^{7+}$	$^{43}\text{Ca}^{19+}$	$^{73}\text{Ge}^{31+}$	$^{131}\text{Xe}^{53+}$	$^{209}\text{Bi}^{82+}$
Leading	143.3127	375.960	657.93	1461.6	4112
QED	-0.0026 (2)	-0.103 (15)	-0.59 (8)	-4.1 (0.8)	-30 (7)
Bohr-Weisskopf	-0.0013 (4)	-0.061 (18)	-0.54 (16)	-8.2 (2.5)	-42 (13)
Quadrupole	-0.0007 (1)	-0.018	-0.42	6.9 (0.1)	7
Recoil	-0.0120	-0.015	-0.02	0.0	0
Total	143.2960 (5)	375.763 (24)	656.36 (18)	1456.3 (2.6)	4046 (15)

The basic angular integrals A_i needed for the evaluation of the Zeeman vertex contribution are given by

$$A_1(\kappa_a, \kappa_b) = \int d\hat{p} \chi_{\kappa_a 1/2}^\dagger(\hat{p}) \sigma_0 \chi_{\kappa_b 1/2}(\hat{p}), \quad (\text{A6})$$

$$A_2(\kappa_a, \kappa_b) = \int d\hat{p} \chi_{\kappa_a 1/2}^\dagger(\hat{p}) i [\vec{\sigma} \times \hat{p}]_0 \chi_{\kappa_b 1/2}(\hat{p}), \quad (\text{A7})$$

$$A_3(\kappa_a, \kappa_b) = \int d\hat{p} \chi_{\kappa_a 1/2}^\dagger(\hat{p}) i [\vec{\sigma} \times \vec{\nabla}_\Omega]_0 \chi_{\kappa_b 1/2}(\hat{p}), \quad (\text{A8})$$

$$A_4(\kappa_a, \kappa_b) = \int d\hat{p} \chi_{\kappa_a 1/2}^\dagger(\hat{p}) i [\hat{p} \times \vec{\nabla}_\Omega]_0 \chi_{\kappa_b 1/2}(\hat{p}). \quad (\text{A9})$$

These integrals are evaluated by using the standard Racah algebra. The results relevant for this work are

$$\begin{aligned} A_1(-1, -1) &= 1, & A_1(1, 1) &= -1/3, & A_1(-1, 2) &= 0, & A_1(1, -2) &= -2\sqrt{2}/3, \\ A_2(-1, 1) &= 2/3, & A_2(1, -1) &= -2/3, & A_2(-1, -2) &= \sqrt{2}/3, & A_2(1, 2) &= -\sqrt{2}/3, \\ A_3(-1, 1) &= 4/3, & A_3(1, -1) &= 0, & A_3(-1, -2) &= 2\sqrt{2}/3, & A_3(1, 2) &= -\sqrt{2}, \\ A_4(-1, -1) &= 0, & A_4(1, 1) &= -2/3, & A_4(-1, 2) &= 0, & A_4(1, -2) &= -\sqrt{2}/3. \end{aligned} \quad (\text{A10})$$

-
- | | |
|---|--|
| <p>[1] H. Häffner, T. Beier, N. Hermanspahn, H.-J. Kluge, W. Quint, S. Stahl, J. Verdú, and G. Werth, Phys. Rev. Lett. 85, 5308 (2000).</p> <p>[2] J. Verdú, S. Djekić, S. Stahl, T. Valenzuela, M. Vogel, G. Werth, T. Beier, H.-J. Kluge, and W. Quint, Phys. Rev. Lett. 92, 093002 (2004).</p> <p>[3] S. Sturm, A. Wagner, B. Schabinger, J. Zatorski, Z. Harman, W. Quint, G. Werth, C. H. Keitel, and K. Blaum, Phys. Rev. Lett. 107, 023002 (2011).</p> <p>[4] S. Sturm, A. Wagner, B. Schabinger, and K. Blaum, Phys. Rev. Lett. 107, 143003 (2011).</p> <p>[5] P. J. Mohr, B. N. Taylor, and D. B. Newell, Rev. Mod. Phys. 80, 633 (2008).</p> <p>[6] S. A. Blundell, K. T. Cheng, and J. Sapirstein, Phys. Rev. A 55, 1857 (1997).</p> <p>[7] H. Persson, S. Salomonson, P. Sunnergren, and I. Lindgren, Phys. Rev. A 56, R2499 (1997).</p> <p>[8] V. A. Yerokhin, P. Indelicato, and V. M. Shabaev, Phys. Rev. Lett. 89, 143001 (2002).</p> <p>[9] S. G. Karshenboim and A. I. Milstein, Physics Letters B 549, 321 (2002).</p> <p>[10] V. M. Shabaev and V. A. Yerokhin, Phys. Rev. Lett. 88, 091801 (2002).</p> <p>[11] K. Pachucki, U. D. Jentschura, and V. A. Yerokhin, Phys. Rev. Lett. 93, 150401 (2004), [(E) <i>ibid.</i>, 94, 229902 (2005)].</p> | <p>[12] K. Pachucki, A. Czarnecki, U. D. Jentschura, and V. A. Yerokhin, Phys. Rev. A 72, 022108 (2005).</p> <p>[13] T. Beier, H. Häffner, N. Hermanspahn, S. G. Karshenboim, H.-J. Kluge, W. Quint, S. Stahl, J. Verdú, and G. Werth, Phys. Rev. Lett. 88, 011603 (2002).</p> <p>[14] N. F. Ramsey, Phys. Rev. 78, 699 (1950).</p> <p>[15] B. Lahaye and J. Margerie, Opt. Commun. 1, 259 (1970).</p> <p>[16] M. G. H. Gustavsson and A.-M. Mårtensson-Pendrill, Phys. Rev. A 58, 3611 (1998).</p> <p>[17] D. L. Moskovkin, N. S. Oreshkina, V. M. Shabaev, T. Beier, G. Plunien, W. Quint, and G. Soff, Phys. Rev. A 70, 032105 (2004).</p> <p>[18] A. Rudziński, M. Puchalski, and K. Pachucki, J. Chem. Phys. 130, 244102 (2009).</p> <p>[19] V. A. Yerokhin, K. Pachucki, Z. Harman, and C. H. Keitel, Phys. Rev. Lett. 107, 043004 (2011).</p> <p>[20] G. Breit, Nature (London) 122, 649 (1928).</p> <p>[21] H. A. Bethe and E. E. Salpeter, <i>Quantum Mechanics of One- and Two-Electron Atoms</i> (Springer, Berlin, 1957).</p> <p>[22] E. A. Moore, Mol. Phys. 97, 375 (1999).</p> <p>[23] N. C. Pyper, Mol. Phys. 97, 381 (1999).</p> <p>[24] N. C. Pyper and Z. C. Zhang, Mol. Phys. 97, 391 (1999).</p> <p>[25] V. G. Ivanov, S. G. Karshenboim, and R. N. Lee, Phys. Rev. A 79, 012512 (2009).</p> <p>[26] V. M. Shabaev, Phys. Rep. 356, 119 (2002).</p> <p>[27] N. J. Snyderman, Ann. Phys. (NY) 211, 43 (1991).</p> |
|---|--|

- [28] V. A. Yerokhin and V. M. Shabaev, Phys. Rev. A **60**, 800 (1999).
- [29] V. A. Yerokhin, P. Indelicato, and V. M. Shabaev, Eur. Phys. J. D **25**, 203 (2003).
- [30] V. A. Yerokhin, K. Pachucki, and V. M. Shabaev, Phys. Rev. A **72**, 042502 (2005).
- [31] V. A. Yerokhin, A. N. Artemyev, V. M. Shabaev, and G. Plunien, Phys. Rev. A **72**, 052510 (2005).
- [32] V. A. Yerokhin and U. D. Jentschura, Phys. Rev. Lett. **100**, 163001 (2008).
- [33] V. A. Yerokhin and U. D. Jentschura, Phys. Rev. A **81**, 012502 (2010).
- [34] V. A. Yerokhin, P. Indelicato, and V. M. Shabaev, Phys. Rev. A **69**, 052503 (2004).
- [35] V. M. Shabaev, K. Pachucki, I. I. Tupitsyn, and V. A. Yerokhin, Phys. Rev. Lett. **94**, 213002 (2005).
- [36] V. M. Shabaev, I. I. Tupitsyn, K. Pachucki, G. Plunien, and V. A. Yerokhin, Phys. Rev. A **72**, 062105 (2005).
- [37] L. Landau and E. M. Lifshitz, *Quantum Mechanics: Non-Relativistic Theory. Vol. 3* (Pergamon Press, Oxford, England, 1977).
- [38] M. E. Rose, *Relativistic Electron Theory* (John Wiley & Sons, New York, 1961).
- [39] V. A. Yerokhin, A. N. Artemyev, T. Beier, G. Plunien, V. M. Shabaev, and G. Soff, Phys. Rev. A **60**, 3522 (1999).
- [40] C. Itzykson and J. Bernard Zuber, *Quantum Field Theory* (McGraw-Hill, New York, 1980).
- [41] U. D. Jentschura, A. Czarnecki, and K. Pachucki, Phys. Rev. A **72**, 062102 (2005).
- [42] A. Bohr and V. F. Weisskopf, Phys. Rev. **77**, 94 (1950).
- [43] A. Bohr, Phys. Rev. **81**, 331 (1951).
- [44] V. M. Shabaev, J. Phys. B **27**, 5825 (1994).
- [45] V. M. Shabaev, M. Tomaselli, T. Kühn, A. N. Artemyev, and V. A. Yerokhin, Phys. Rev. A **56**, 252 (1997).
- [46] O. M. Zhrebtsov and V. M. Shabaev, Can. J. Phys. **78**, 701 (2000).
- [47] L. Elton and A. Swift, Nucl. Phys. **A94**, 52 (1967).
- [48] E. Rost, Phys. Lett. **26B**, 184 (1968).
- [49] I. Angeli, At. Data Nucl. Data Tables **87**, 185 (2004).
- [50] P. Raghavan, At. Data Nucl. Data Tables **42**, 189 (1989).
- [51] N. J. Stone, At. Data Nucl. Data Tables **90**, 75 (2005).